Understanding the electro-chemo-mechanics of lithium metal anodes

eScience 6 (2026) 100429

Contents lists available at ScienceDirect

eScience

journal homepage: www.keaipublishing.com/en/journals/escience

Review

Understanding the electro-chemo-mechanics of lithium metal anodes

Quan Wu[a], Elin Dufvenius Esping[a], Marita Afiandika[a,c], Shizhao Xiong[a,b,*], Aleksandar Matic[a,c,*]

[a] Department of Physics, Chalmers University of Technology, Gothenburg, 41296, Sweden
[b] Faculty of Material Science and Engineering, Kunming University of Science and Technology, Kunming, 650093, China
[c] Wallenberg Wood Science Center, Chalmers University of Technology, Gothenburg, 41296, Sweden

HIGHLIGHTS

- Electrochemical plating/stripping of Li is coupled electro-chemo-mechanics process.
- Uniform plating of Li is dependent on factors of substrate, electrolyte and condition.
- Integrating experiment with theory are essential for future lithium metal batteries.

GRAPHICAL ABSTRACT

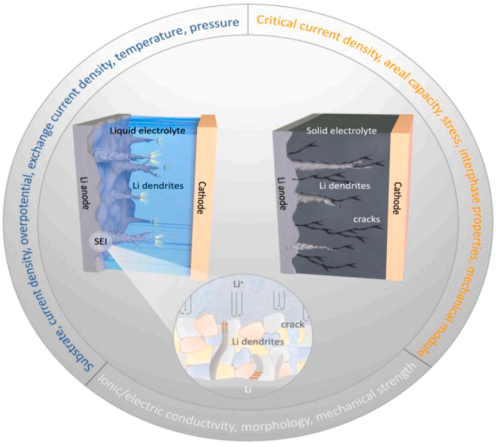

ARTICLE INFO

Keywords:
Lithium metal batteries
Electro-chemo-mechanics
Multiphysics
Solid–electrolyte interphase
Solid-state electrolyte

ABSTRACT

Lithium metal batteries (LMBs) are candidates for next-generation energy storage due to their potential to increase energy density. However, the nonuniform electrodeposition of Li during cycling, plus the growth of Li dendrites and the side reactions between Li metal and the electrolyte, hinder the practical deployment of LMBs. The plating/stripping behavior of Li is an electro-chemo-mechanical process, and gaining a thorough understanding of its mechanisms is a cornerstone of LMB development. In this review, the current understanding of electro-chemo-mechanical processes on Li metal anodes is systematically summarized from the perspectives of Li plating/stripping in liquid- and solid-state electrolytes, the important role of the solid–electrolyte interphase, and the methodologies for understanding the electro-chemo-mechanics of the Li metal anode. The aim is to promote the development of LMBs through the optimization of Li metal anodes, which is based on understanding the fundamental processes occurring during electrochemical plating and stripping.

* Corresponding authors.
E-mail addresses: shizhao.xiong@kust.edu.cn (S. Xiong), matic@chalmers.se (A. Matic).
Peer review under the responsibility of Editorial Board of eScience.

https://doi.org/10.1016/j.esci.2025.100429
Received 12 January 2025; Received in revised form 9 March 2025; Accepted 11 May 2025
Available online 16 May 2025

1. Introduction

Batteries with higher energy density are ongoing goals for both the academic community and industry, due to the ever-increasing demands for a longer driving range in electric vehicles, large-scale energy storage, and new applications such as electric aviation. Lithium metal batteries (LMBs) are a potential solution due to their high theoretical specific capacity (3860 mAh g^{-1}) and the low redox potential (−3.04 V vs. SHE) of Li metal, which are key features for high energy density cells [1,2]. However, the practical deployment of LMBs is impeded by nonuniform Li plating/stripping, uncontrollable Li dendrite formation, inactive Li, and side reactions at the Li metal/electrolyte interface, which result in capacity fade, decreased Coulombic efficiency, increased overpotential, gas release, or short-circuiting [3].

An in-depth and comprehensive understanding of the Li metal anode's mechanisms is a prerequisite for addressing these issues and developing LMBs with high energy density, a long life span, and safety. The performance of Li metal anodes is highly determined by the electrochemical plating and stripping processes, which are controlled by electrochemical parameters such as current density, overpotential, and ionic transport kinetics, among others. In parallel, the Li metal anode is affected by the internal mechanics of the Li substructure and by external mechanics such as the mechanical modulus of the substrate, the solid electrolyte interphase (SEI), and the solid-state electrolyte (SSE). Therefore, the mechanisms of the Li metal anode can be viewed and described as coupled electro-chemo-mechanical processes [4,5].

Comprehending these processes requires a detailed discussion of the Li plating reactions. The plating of Li can be divided into two main steps: Li nucleation and the growth of Li structures. Initially, Li ions in the electrolyte migrate towards the electrode surface, are reduced, and can form nuclei when the local overpotential exceeds the surface energy. The Li ions that subsequently reach the electrode surface will preferentially plate on the nuclei, leading to the early growth of Li structures [6]. Thus, the plating behavior is largely affected by electrochemical parameters, the mechanical modulus of the substrate, and external factors like temperature and pressure. For example, current density influences the size of nuclei and the microstructural evolution during the growth phase [7]. SEIs with different Young's modulus values have varying effects on nucleation due to the differences in sustained inner pressure [8]. Temperature and pressure, on the other hand, affect Li plating by changing the ion diffusion in the electrolyte, the desolvation kinetics, and the preferential plating of Li [9,10]. These electrochemical and mechanical parameters interact and jointly control the behaviors of the Li metal anode. Therefore, a holistic approach that considers all factors systematically is necessary and can be applied by taking an electro-chemo-mechanical approach.

As already noted, the electrochemical potential of Li is −3.04 V vs. SHE, which is a double-edged sword. On the one hand, low potential is a prerequisite for obtaining a high cell voltage and energy density. On the other hand, a potential this low is outside the electrochemical stability window of most electrolyte formulations, leading to side reactions between Li and the electrolyte during plating. Ideally, this results in the formation of a passivation layer, the SEI, which can stabilize the electrode/electrolyte interface [11]. During plating, Li ions need to be transported through the SEI and then plate beneath it [1]. Hence, the nature of the SEI has a substantial influence on the plating behavior. Most important are: 1) mechanical properties: the SEI needs to have sufficient Young's and elastic moduli to accommodate volume expansion and avoid the SEI cracking during Li plating; 2) chemical composition: an SEI composed of mainly inorganic compounds such as LiF has higher ionic conductivity and mechanical strength, mitigating stress concentration after Li plating; 3) electronic conductivity: a SEI with high electronic conductivity not only leads to poor passivation of the interface due to consistent reduction of the electrolyte and the accumulation of side products but also induces hot spots for Li dendritic growth; 4) ionic conductivity: a SEI with high ionic conductivity facilitates fast Li-ion transport, guaranteeing uniform Li plating; 5) uniformity: a nonuniform SEI leads to heterogeneous ionic and electronic conductivities, and increased ion/electron transport in domains with high conductivity leads to the formation of hot spots and nonuniform Li plating; and 6) morphology: a thin, dense SEI mitigates side reactions between the electrolyte and the Li electrode [12]. The ideal SEI should therefore be thin, dense, mechanically robust, conductive to Li ions, and insulating to electrons, so it is important for these properties to be tunable to obtain uniform Li plating [13]. SEI properties are to a large extent determined by the electrolyte composition and physical properties. Hence, electrolyte engineering is an effective way to manipulate the nature of the SEI and battery performance.

In this review, we present a systematic summary of the electro-chemo-mechanical coupled process of Li plating and discuss the interplay between the SEI and Li plating. We also introduce some key advanced characterization methods for studying Li plating and offer perspectives and directions for the future development of Li metal anodes.

2. Electro-chemo-mechanics of Li metal anodes in liquid-state electrolytes

Li plating is a complicated process but can be divided into early Li nucleation and Li growth. From the perspective of thermodynamics, at the beginning of nucleation, Li ions from the electrolyte are driven by the electric field to adsorb on the substrate surface and form adatoms when the overpotential exceeds the surface energy. Subsequently, Li ions are reduced to Li metal and form embryos with chemical bonds to the surface atoms; this process is controlled by the lithiophilicity of the substrate (Fig. 1a) [14], which is determined by the binding energy between Li and the atoms on the substrate surface, as well as by the substrate's surface energy. The overpotential, current density, and external parameters such as temperature and pressure also influence the nucleation of Li and the growth of the substructure.

2.1. Substrate

Zhang et al. used first-principles calculations to investigate the lithiophilicity of different heteroatom-doped carbon surfaces and its influence on Li nucleation [15]. The results show that three factors affect lithiophilicity: the electronegativity of the dopants, the local dipole between the doping atom and adjacent carbon, and charge transfer. The electronegativity affects the binding energy according to Lewis acid–base theory [15]. The increased local dipole improves lithium's anchoring effect due to the enhanced ion-dipole force. There is a critical charge transfer value of 0.9 e^-, below which the binding energy is too small [15]. A higher binding energy and a lower surface energy lead to stronger substrate lithiophilicity, resulting in a lower nucleation overpotential, which contributes to a uniform and dense Li plating morphology [16].

After the adsorption of Li ions on the substrate and the formation of adatoms, the Li nuclei form by the aggregation of Li adatoms, followed by the growth of substructures. Jiao et al. used phase-field modeling to study the self-diffusion barrier of Li adatoms based on four different metal substrates (LiAg, LiMg, Cu/Ni, and Li) [14]. The results indicate that a lower self-diffusion barrier accompanied by a faster self-diffusion of Li adatoms leads to larger Li nuclei, as well as Li substructures with a lower aspect ratio and, consequently, more uniformly plated Li. As shown in Fig. 1b, the LiAg substrate has a low self-diffusion barrier and a high hopping rate, which promote uniform Li plating.

In addition to the manipulation of substrate composition to promote uniform Li plating, it is also important to control the substrate morphology, e.g., by building a 3D framework structure to accommodate the volume change and induce dense, even Li plating. Ding et al. proposed a 3D porous structure, with a lithiophilic CuSnAl layer on top of a Cu foam (Fig. 1c) [17]. This substrate supported reversible Li plating over 2000 h at 1 $mAcm^{-2}$ [17].

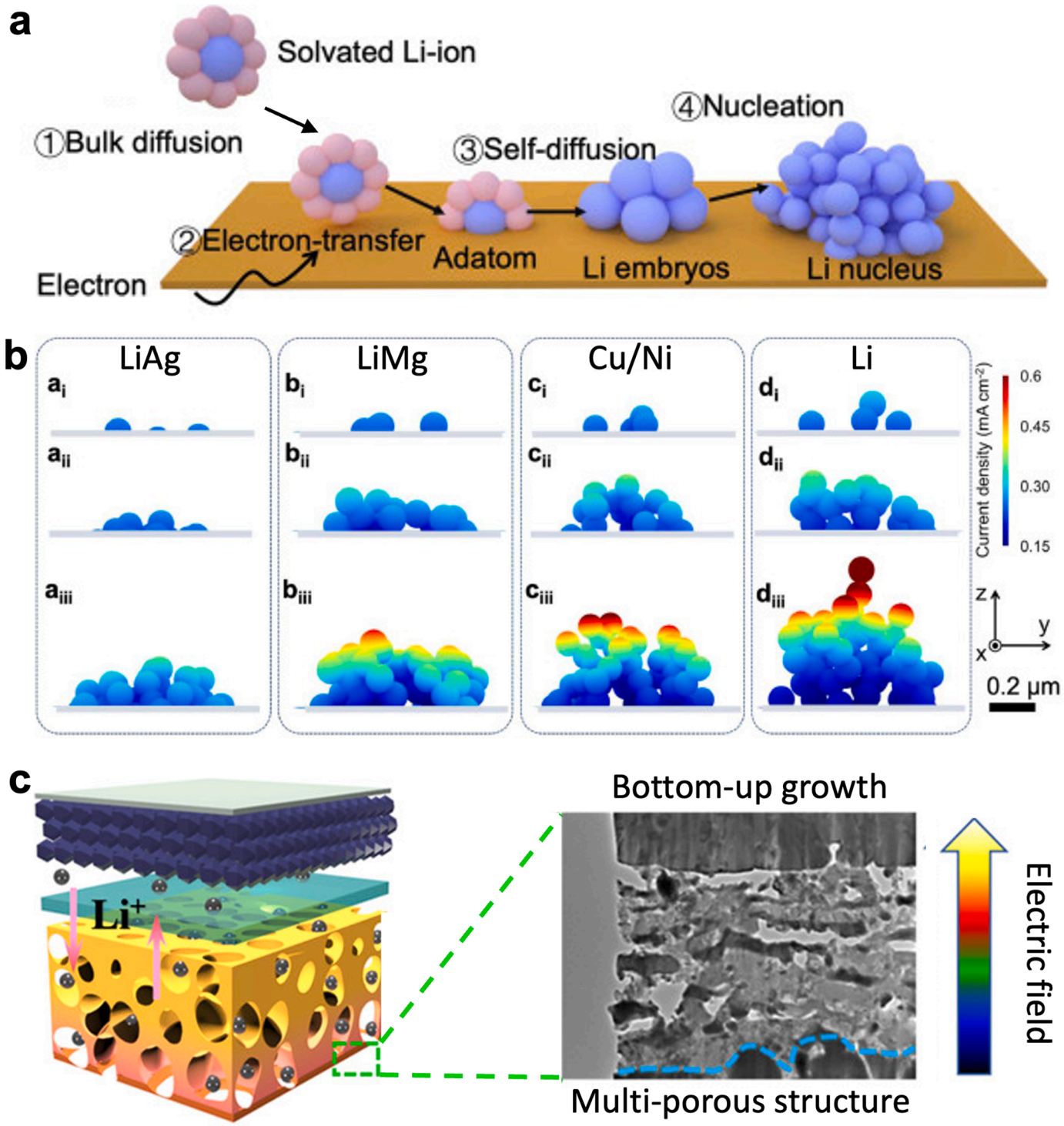

Fig. 1. (a) Schematic of nucleation during Li plating [14]; (b) Li substructures based on growth of Li nuclei on different substrate surfaces [14]; (c) schematic of the CuSnAl@Cu foam structure, and cross-sectional TEM image of its bottom zone [17] (Reproduced from Ref. 17 with permission from American Chemical Society).

2.2. *Current density and overpotential*

Current density and overpotential determine the kinetics and play a vital role in Li plating/stripping. The process of Li plating is a combination of mass transport in the liquid-state electrolyte (LSE) and interfacial charge transfer. When a current flows through a battery to recharge it, solvated Li ions are transported to the electrolyte/electrode interface and shed their solvation shells, then Li ions accept electrons, are reduced to metallic Li, and plate on the substrate. Consequently, cations are consumed at the interface and anions are expelled, driven by the electric field [3]; this creates a concentration gradient in the electrolytic salt near the electrode surface, which is controlled and described by a diffusion equation [18]. For currents greater than the diffusion limit, the salt concentration at the electrode surface becomes zero after a given time, and the electrolytic fluid turns to dielectric fluid, causing unstable and inhomogeneous Li plating. Sand labeled this characteristic time "Sand's time" (τ_s) in 1901 [19]; after this point, Li plating will preferentially occur on surface protrusions with higher salt concentrations to maintain the electroneutrality, culminating in dendritic development [18].

Bai et al. studied the different formation mechanisms of mossy and dendritic Li by observing the growth process in a glass capillary cell [18]. They found that mossy Li growth is a reaction-limited process, while dendritic Li growth is transport limited. As shown in Fig. 2a, when a constant current density is used, mossy Li plates tend to root-grow at the beginning of Li plating. With continued Li plating, the salt concentration near the substrate surface decreases, and with the depletion of salt, dendritic Li suddenly shoots out, which is evidence of tip growth. The experimental Sand's time was accurately measured via this visualization of Li plating, whereby an apparent diffusion coefficient D_{app} could be calculated from Sand's formula. The limiting current density was derived as $J_{lim} = 2z_c c_0 F D_{app}(t_a L)^{-1}$, where z_c is the charge number of the cation, c_0 is the bulk salt concentration, F is Faraday's constant, t_a is the transference number of anions, and L is the distance between the electrodes. If current density $J < J_{lim}L$ in a finite L system, no tip-grown dendrites will occur; if $J > J_{lim}$, tip-growth dendritic Li will shoot out within Sand's time. Based on this formula, an electrolyte with a high salt concentration and a low anion transference number is desirable for a longer Sand's time and to suppress Li plating instabilities. For instance, in an electrolyte of 1 M $LiPF_6$ ethylene carbonate (EC) and dimethyl carbonate (DMC) (volume ratio of 1:1), when the distance between the two electrodes is 5 mm, the J_{lim} was calculated to be 1 mA cm^{-2}, which was consistent with experimental observation. Bai et al. also defined Sand's capacity (C_s) based on Sand's time theory, $C_s = J\tau_s$, as shown in Fig. 2b, which provides a simple design constraint to avoid dendritic lithium [18].

Sadd et al. investigated the influence of current density on the morphology of plated Li by operando X-ray tomographic microscopy (XTM) [7]. The results show that at a low current density (0.5 mA cm^{-2}), needle-like Li microstructures predominate due to preferential plating at the kinks of the needle-like structures. This type of microstructure shows low reversibility during stripping, leading to electric disconnection and the formation of inactive Li (Fig. 2c left). When a high current density (1 mA cm^{-2}) is applied in the second cycle, moss-like Li microstructures are observed due to the relatively smaller nucleation overpotential, providing better reversibility than the needle-like Li (Fig. 2c right) [7]. In particular, needle-like and mossy Li form simultaneously at high current densities, and the increased current density leads to the rapid growth of Li structures, with current hot spots at the tip of these structures boosting the risk of short circuits.

Although high current densities were previously believed to induce dendrite formation, Li et al. found that dendrites self-heated at current densities exceeding 9 mA cm^{-2}. They conducted both experimental and theoretical studies and concluded that Joule heating of dendrites might cause substantial Li diffusion, allowing the densely packed dendritic particles to combine and smooth the Li metal surface [20]. Yuan et al. discovered that ultrahigh current (50–1000 mA cm^{-2}) allows for the non-dendritic growth of Li rhombic dodecahedra when no SEI is present. They concluded that the morphology of non-dendritic Li deposits during ultrafast Li deposition is independent of the electrolyte chemistry and the current collector material. This was because they eliminated the mass transport limitation by utilizing an ultramicroelectrode (d = 25–255 μm), and ultrahigh currents lead to Li deposition that overcomes SEI development [21].

Pei et al. investigated the relationship between plated Li morphology and overpotential/current density. Overpotential is the driving force of nucleation; a smaller overpotential corresponds to faster self-diffusion of Li^+ ions, which promotes a tendency toward lateral growth that leads to larger-sized Li nuclei. The surface growth of Li is dominant in the Li plating reactions, rendering a more macroscopically compact Li plating morphology. In contrast, the larger overpotential, accompanied by a high current density, generates slow Li diffusion kinetics, in which tip growth takes the place of surface growth, and Li tends to plate vertically rather than laterally, leading to the growth of Li dendrites. Thus, increased current density and overpotential decrease the size but increase the number of nuclei (Fig. 2d) [22]. Exchange current density is related to the intrinsic kinetics of Li^+. Lower exchange current density is correlated to lower overpotential, facilitating uniform and dense Li plating with larger Li nuclei, which suppresses the growth of Li dendrites and contributes to a high Coulombic efficiency (Fig. 2e) [16]. In contrast, a high exchange current density leads to needle-like Li plating and the growth of Li dendrites [16].

The formation of "dead" Li also influences the performance of Li-metal anodes. During stripping, a part of a Li dendrite may lose its electric connection to the current collector and therefore become isolated, forming "dead" Li. This occurs due to the fast stripping of Li from the dendrite at high current densities (Fig. 2f). In addition to fast stripping, rapid SEI formation can lead to the insulation of Li structures and the formation of "dead" Li (Fig. 2g) [23].

2.3. Temperature and pressure

Temperature plays an important role in Li plating by influencing the reaction kinetics as well as Li-ion transport through the electrolyte and SEI. McDowell et al. studied the influence of temperature on Li plating and showed that decreased temperature leads to slow Li transport kinetics, resulting in increased overpotential; this causes a greater density of smaller Li nuclei, which correlates to an increased overpotential [24].

Li plating is also substantially affected by the applied pressure. Increased pressure alleviates the formation and growth of Li dendrites and promotes the plating of Li in densely packed, larger grains with a smooth surface. As reported by Fang et al., the pressure changes the free energy of the substrate surface, inducing the lateral growth of Li along the surface in the early stages [10]. Only after Li has covered the surface does the plating begin to grow vertically, forming dense, columnar structures. Thus, the application of pressure promotes compact plating and decreases the porosity of plated Li, which might minimize volume expansion during cycling [10].

Meng et al. used a mechano-electrochemical phase field model to study the influence of pressure on Li plating, and designed a pressure control apparatus (Fig. 3a) to experimentally investigate pressure-controlled Li plating [25]. With increasing external pressure, the local hydrostatic pressure in Li dendrites changes from negative to positive, which means there is a shift from expansion to contraction. When the external pressure reaches 14 MPa, the hydrostatic pressure at the Li dendrite tip reaches a peak value (20 MPa), so growth at the tip is inhibited and transfers to lateral growth (Figs. 3b and c) [26]. However, an upper limit on the external pressure should be considered, since if the applied pressure exceeds the yield strength, the electrode material and separator might crack; the Li dendrites might also crack and fracture, thereby losing their electric contact and forming inactive Li. Hence, applying a high external pressure that stops below the yield strength facilitates the formation of dense, smooth, and columnar plated Li, which promotes high Coulombic efficiency for LMBs.

Besides external pressure, the internal stress induced by plated Li also influences the plating process. Wang et al. reported that the application of a soft substrate can relieve compression stress resulting from Li plating. During plating, compressive stress accumulates and is transferred to the current collector, leading to wrinkling when the stress reaches the membrane's strain threshold. By using a soft substrate, the stress in plated Li can be relieved, rendering uniform Li plating. A soft PDMS-composed Cu current collector is applied to support surface wrinkling; the 2D structure of this wrinkling can reduce the stress in the plated Li structure. The relaxation of stress suppresses the stress-driven root growth of Li whiskers to promote dense, uniform Li plating (Figs. 3d and e) [27].

In summary, as shown in Fig. 4, the plating and stripping of Li are electro-chemo-mechanical processes, which are controlled by parameters such as overpotential, current density, exchange current density, temperature, and internal/external pressure. Dense, mossy Li growth is preferential, since it is more reversible during plating/stripping, which facilitates long cycle life. The morphology of plated Li is highly

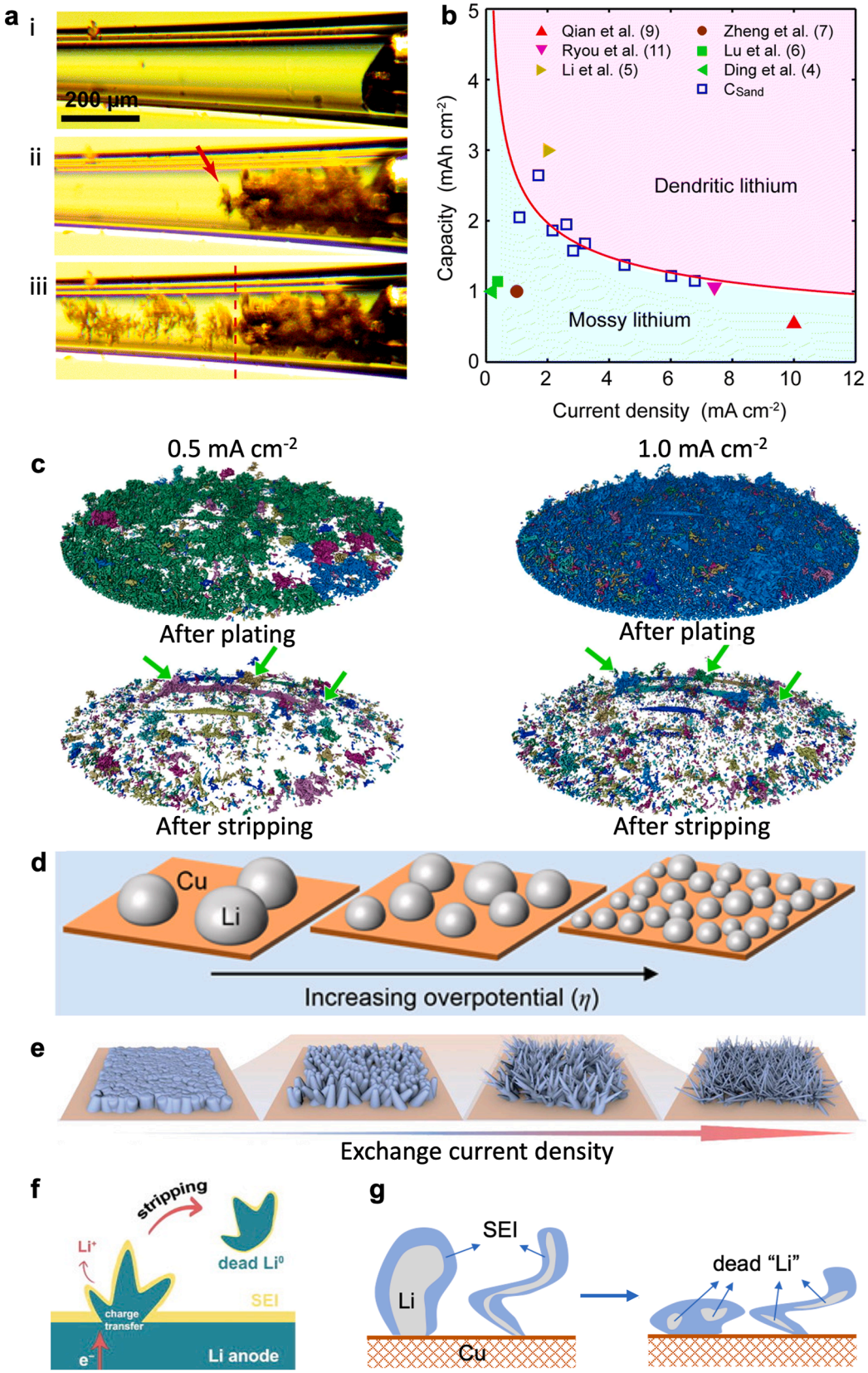

Fig. 2. (a) *In situ* snapshots of the growth of Li during electroplating. Red arrow in (ii) points to the emergence of dendritic Li. Red dashed line in (iii) labels the morphological difference between the pre- and post-Sand's time Li plating; (b) Sand's capacity versus current density [18] (Reproduced from Ref. 18, with open access from the Royal Society of Chemistry); (c) Li plating morphologies by rendering of tomograms taken after plating and stripping at different current densities of 0.5 and 1.0 mA cm^{-2} [7]; (d) schematic illustrating the size and density of Li nuclei plated on Cu at varying overpotentials [22] (Reproduced from Ref. 22 with permission from American Chemical Society); (e) schematic of electroplating of Li under different exchange current densities [16]; (f) schematic of "dead" Li formation during Li stripping [23]; (g) schematic of the formation of "dead" Li during fast SEI formation [23] (Reproduced from Ref. 23 with permission from Elsevier).

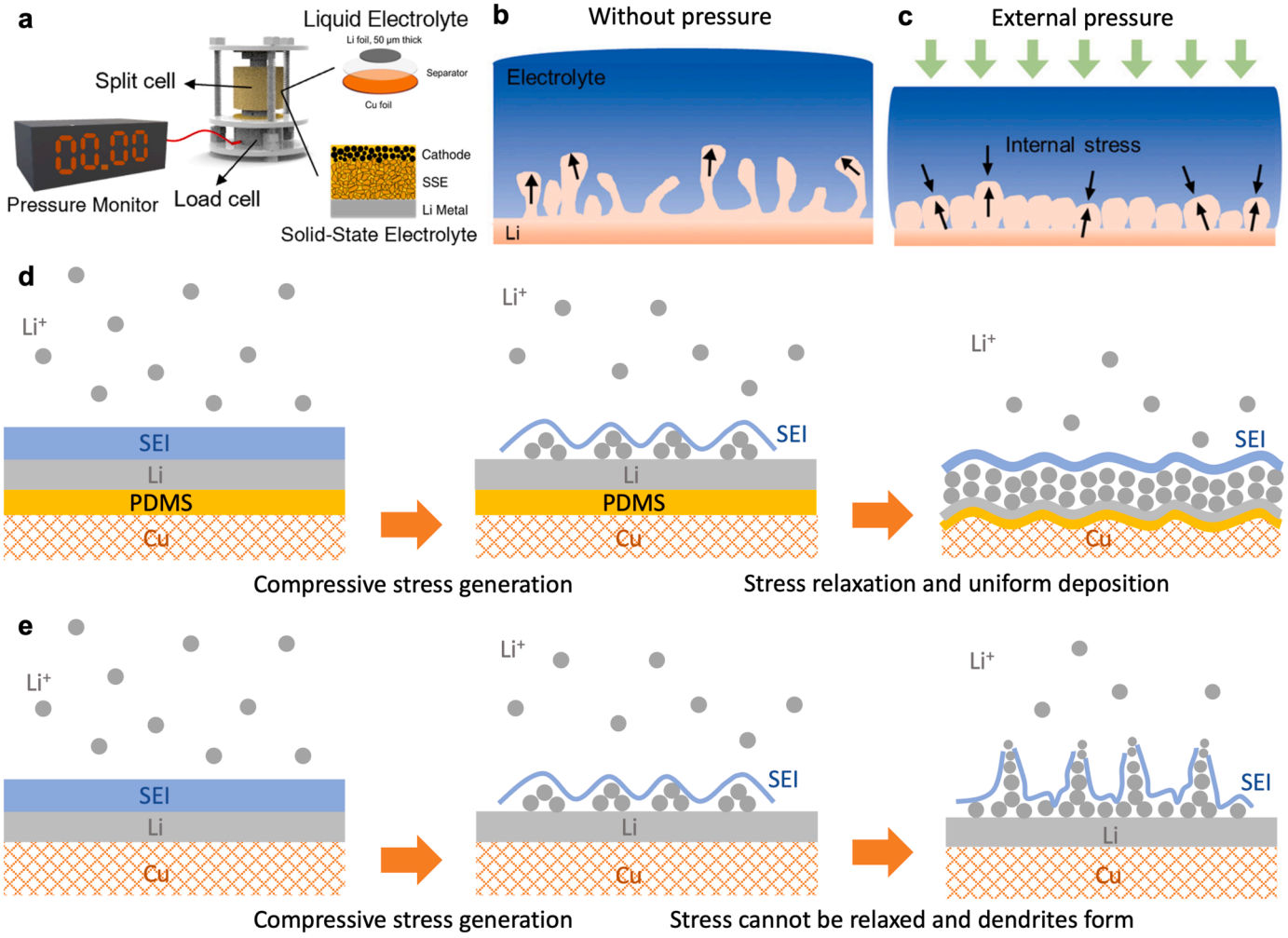

Fig. 3. (a) Pressure control apparatus for LMB with liquid electrolyte or solid-state electrolyte [25] (Reproduced from Ref. 25 with open access from the Electrochemical Society); (b) schematic illustration of the morphology of Li dendrites without and (c) with external pressure [26] (Reproduced from Ref. 26 with permission from Wiley); (d) mitigation of Li dendrite formation by releasing compressive stress using a soft substrate; (e) formation of Li dendrites due to Li-plating-induced compressive stress using a hard substrate, e.g. Cu foil.

dependent on the early nucleation behavior. In general, the following principles apply: 1) a lower nucleation overpotential and current density lead to larger nuclei and a lower density of nuclei, contributing to uniform, dense Li plating that suppresses Li dendrite growth; 2) a smaller overpotential, corresponding to a smaller exchange current density, guarantees a low aspect ratio in the plated Li structure; 3) the faster Li^+ ion transport kinetics resulting from high temperature decreases the nucleation overpotential, which facilitates homogenous Li plating. After the early nucleation stage, the internal stress of the Li structure accumulates with the growth of Li, leading to tip growth. The application of external pressure can effectively suppress tip growth in favor of lateral growth. In addition, exploiting soft substrates can relieve internal stress and lead to uniform Li plating. The formation of "dead" Li results in irreversible Li consumption and low Coulombic efficiency. Moreover, the accumulation of inactive Li gives rise to safety risks and greater cell resistance.

3. Electro-chemo-mechanical function of SEI on Li metal anode

The SEI forms as soon as the electrolyte is in contact with Li metal, and it continues to form during the initial cycles until the Li metal anode is completely passivated by the SEI [12]. The desolvated Li^+ ions transport through the SEI and nucleate; therefore, the Li plating and stripping behavior is influenced by the SEI's properties, including ionic/electric conductivities, homogeneity, mechanical strength, and thickness. So a SEI with high ionic conductivity leads to fast ionic diffusion kinetics through the SEI, resulting in a uniform distribution of ionic flux and Li plating. However, high electric conductivity results in current hot spots and continuous side reactions between the Li metal anode and the electrolyte, which lower the cycling stability [8]. A SEI with reasonable mechanical strength can suppress Li tip growth and the formation of Li dendrites by homogenizing the internal stress of the Li structure. If the formed SEI is porous and inhomogeneous, the reaction between electrolyte and Li metal can proceed to continuously thicken the SEI, causing irreversible Li depletion, decreased Coulombic efficiency, and increased cell resistance. Hence, a thin, dense, and homogenous SEI with sufficient ionic conductivity, mechanical strength, and low electric conductivity is favorable. Manipulating the properties of the SEI can effectively control the plating and stripping of Li and consequently the LMB's performance.

3.1. Ionic conductivity and chemical composition

The ionic conductivity of the SEI affects the plated Li morphology by controlling the ionic diffusion kinetics. During the process of Li plating, Li ions de-solvate in the vicinity of the SEI and are transported through it. Subsequently, Li ions adsorb on the substrate and are reduced to metallic Li, accompanied by electron transfer; this is followed by Li

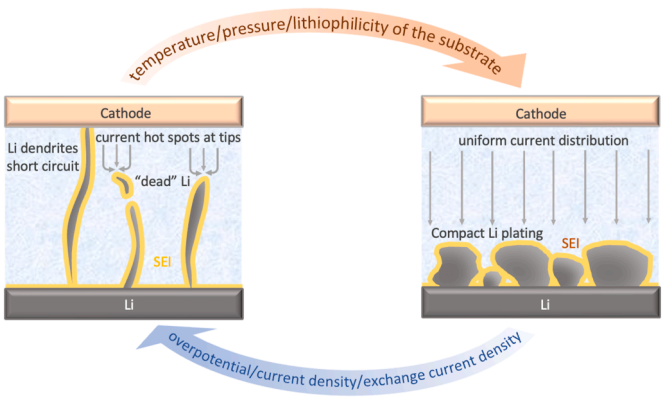

Fig. 4. Schematic of the electro-chemo-mechanics of Li metal anodes in LSEs.

nucleation and early growth beneath the SEI (Fig. 5a) [13]. Thus, a low ionic conductivity leads to localized Li plating and dendritic growth, causing stress concentration because dendritic plating is a diffusion-controlled process, as discussed previously. As shown in Fig. 5b, a mosaic-like SEI — composed of different compounds (for example, LiF, $LiCO_3$, etc.), with various ionic conductivities, thicknesses, chemical properties, or mechanical moduli — leads to inhomogeneous ion flux and nonuniform Li plating as well as dendrite growth [8,12].

Hao et al. used density functional theory calculations to study Li surface diffusion kinetics and Li plating behavior based on two primary components of the SEI: LiF and Li_2O. As illustrated in Fig. 5c, the SEI suffers from bending and stretching during plating due to volume expansion. In regions of LiF that experience stretching, Li adatoms show higher diffusion rates, which inhibits the accumulation of Li ions in these regions and thus prevents Li dendrite growth. However, for Li_2O, the diffusion rate of Li adatoms is lower in regions experiencing stretching, resulting in accelerated dendritic growth [28]. Therefore, a SEI with fast surface diffusion kinetics facilitates uniform plating and suppresses dendritic Li growth. This work clarifies the influence of different components of the SEI on the ionic diffusion kinetics and Li plating, which also signifies the importance of SEI homogeneity.

3.2. Mechanical strength

Stress accumulation under the SEI affects the Li plating, which is a mechanics-dominated process. Kushima et al. proposed a stress-controlled root growth mode for the relation between the SEI and the Li plating morphology [29]. As illustrated in Fig. 5d, during the early stages of nucleation on the substrate (stage 1), a thin SEI covers the spherical nuclei, hindering further surface growth. Stress builds up beneath the SEI during continuous growth, and when the stress reaches a threshold, the SEI breaks. A Li whisker shoots out from the root and pushes the formerly plated Li away from the substrate (stage 2). After relaxation of the stress, the Li whisker growth slows down (stage 3). The next whisker grows (stage 4) due to the repetition of stages 2 and 3, when the stress again accumulates. During stripping, the root-grown Li whisker is fragile and the newly formed SEI on this part is thin, so the Li close to the root dissolves first, leading to electric disconnection of the top of the Li whisker, forming "dead" Li as a result.

The accumulation of stress beneath the fragile SEI will also cause it to crack and expose fresh Li metal to the electrolyte, forming a new SEI. During this process, the active Li becomes isolated from the electrolyte again. This process is called "self-healing," but it also results in fast ion-diffusion channels (Li flooding), inducing localized Li dendrite growth at these hot spots. Repeated "self-healing" leads to the consumption of electrolyte and active Li, causing electrolyte depletion and low Coulombic efficiency [12]. A robust SEI with high mechanical strength can endure the stress induced by volume expansion, therefore inhibiting SEI cracking. Based on finite element modeling, Shen et al. proposed that an elastic modulus of 3.0 GPa is enough for a mechanically stable SEI.

Constructing an artificial SEI is an effective route for manipulating the Li morphology by controlling the uniformity, components, and mechanical strength of the SEI. Liu et al. built an electro-chemo-mechanical model to understand the relationship between the physical properties of an artificial SEI and plated Li morphology. The results show that the high ionic conductivity of the SEI is a prerequisite for uniform Li plating, as it provides homogenous ion flux and decreasing compressive stress. They also proposed a Young's modulus of 4.0 GPa as a threshold for achieving even Li plating, with uniform distribution of the von Mises stress and the electrochemical field (Fig. 5e) [8].

Dong et al. proposed a part-substitution carboxymethylcellulose Li as an artificial SEI with a high Li-ion transference number, high Young's modulus, and good lipophilicity, which showed good adaption to volume changes, enabling dense and uniform Li plating [11]. Zhao et al. proposed a new strategy for manipulating Li plating by constructing a dual-layer artificial SEI, where the outer layer is organic and the inner layer is Al_2O_3. The organic layer is porous and flexible and can accommodate volume expansions during Li plating, as well as facilitate electrolyte infiltration. The inner inorganic layer is dense, which prevents side reactions between the electrolyte and the Li metal anode [30].

3.3. Electrolyte engineering

Manipulating SEI properties by electrolyte engineering is an effective strategy to electrochemically control Li plating, since the SEI is composed of the side reaction products between the Li metal anode and the electrolyte. The physicochemical properties of the SEI are highly dependent on the electrolyte composition (solvents, additives, and concentration of Li salts), which determines the solvation structure and the electrolyte stability.

For traditional commercial electrolytes with carbonate solvents (for example, propylene carbonate (PC)), Li ions coordinate primarily with organic molecules due to the high polarity of carbonates, inducing a fragile, organic-rich SEI with high ionic diffusion barriers, leading to nonuniform ion flux and dendritic growth [31].

Substitution of ester-based solvents with ether-based solvents that have weak polarity and more resistance to reduction decreases the proportion of organic molecules in the solvation shell and leads to a thinner, inorganic-rich SEI, which facilitates uniform Li plating and higher Coulombic efficiency. The formation of flexible oligomers in the SEI due to the application of ether-based electrolytes also improves the SEI's stability and flexibility, overcoming the issues of electrolyte decomposition and Li dendrite growth [32].

Introducing additives is also a useful technique to improve the SEI. Fluoroethylene carbonates (FEC) are fluorinated additives that produce a LiF-rich SEI with a high surface energy and a low ionic diffusion barrier, resulting in uniform Li-ion flux and even Li plating [33]. Vinylene carbonate (VC) is easily polymerized on the Li surface, leading to the formation of long-chain hydrocarbon components, which is advantageous for creating a flexible and stable SEI [31]. Electrolytes with lithium bis(oxalato)borate (LiBOB) as an additive help promote even Li plating by forming fibrous Li surfaces instead of dendritic Li growth [34]. Lithium difluoro(oxalate)borate (LiDFOB) can also improve the thermal stability of the electrolyte and form a stable SEI [35]. Textured and uniform Li plating with spherical Li particles was obtained by adding $LiNO_3$ to an ether-based electrolyte [36]. The addition of $LiNO_3$ also leads to the formation of Li_3N in the SEI, which is favorable for improving ionic conductivity [37].

Highly concentrated electrolytes have been considered an effective route to obtain desirable Li plating. The high salt concentration leads to more anions participating in the solvation structure, forming inorganic-rich SEIs; this not only increases the Li-ion transference number but

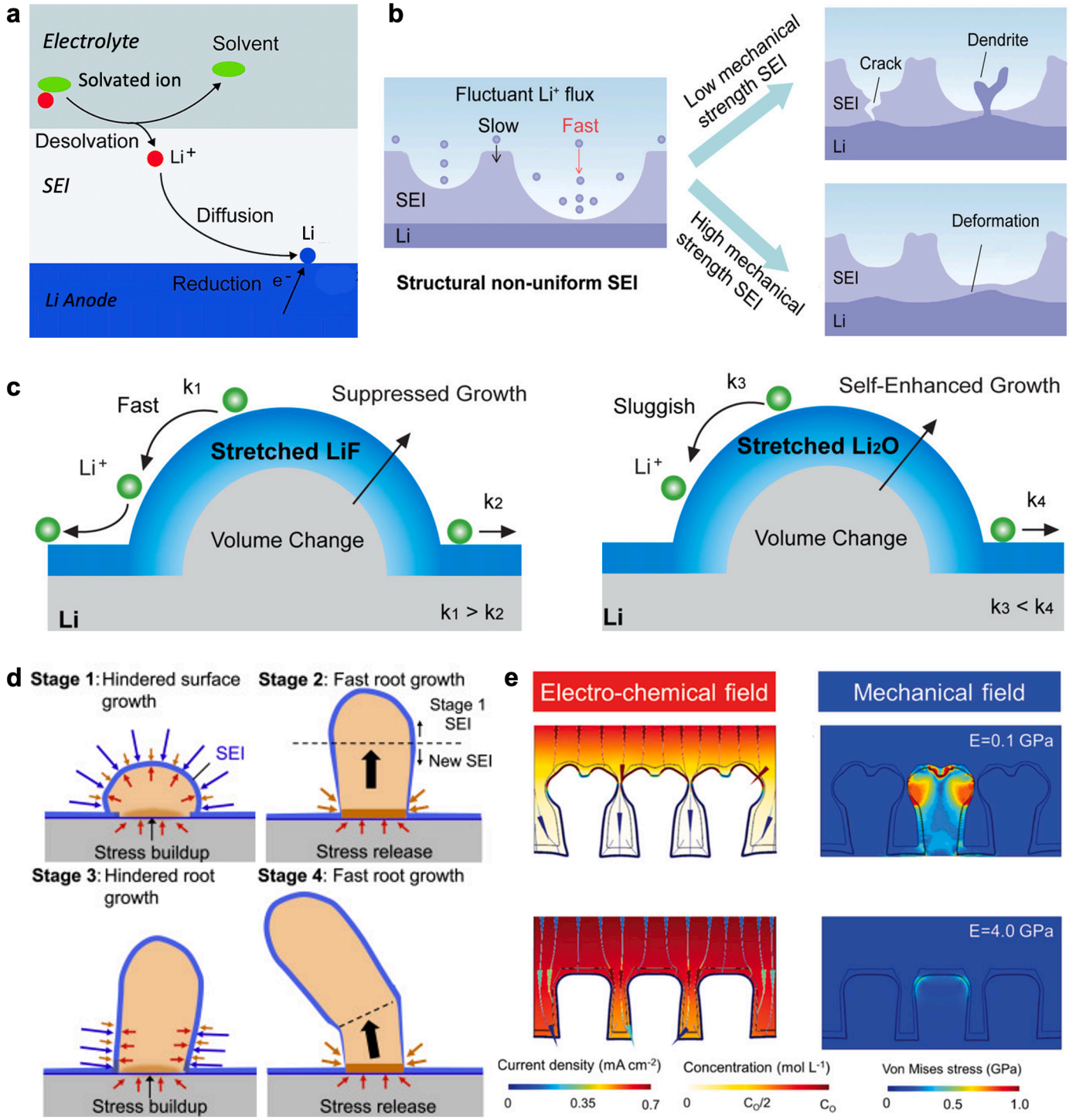

Fig. 5. (a) Schematic of Li electroplating on a Li metal anode surface [13] (Reproduced from Ref. 13 with permission from Royal Society of Chemistry); (b) a nonuniform SEI yields irregular Li plating and crack formation under low mechanical strength, and sustains deformations under high mechanical strength [12] (Reproduced from Ref. 12 with permission from Wiley); (c) surface diffusion on a stretched LiF and Li_2O surface [28] (Reproduced from Ref. 28 with permission from American Chemical Society); (d) schematic illustration explaining the root growth mechanism of lithium whiskers [29] (Reproduced from Ref. 29 with permission from Elsevier); (e) distribution of physical fields on electrodeposited Li covered by SEI with a Young's modulus of 0.1 and 0.5 GPa [8].

also suppresses diffusion-limited Li dendrite growth and yields a high Coulombic efficiency [38]. However, concentrated electrolytes have high viscosity and density, which decrease the LMB's electrochemical performance. Introducing weakly polar solvents, such as bis(2,2,2-trifluoroethyl) ether (BTFE), as diluents to form localized highly concentrated electrolytes reduces the viscosity but preserves the anion-rich solvation structure [39,40]. Lee et al. observed the Li plating morphology by cryo-focused ion beam (cryo-FIB) in a conventional ester-based electrolyte (1.0 M LiPF6 EC/EMC 3:7 (Gen II)), a single salt highly concentrated electrolyte (4.6 M LiFSI-DME (SSEE)), and a bisalt highly concentrated electrolyte (4.6 M LiFSI + 2.3 M LiTFSI in DME (BSEE)) [41]. As shown in Fig. 6a, Li plated in Gen II is porous and

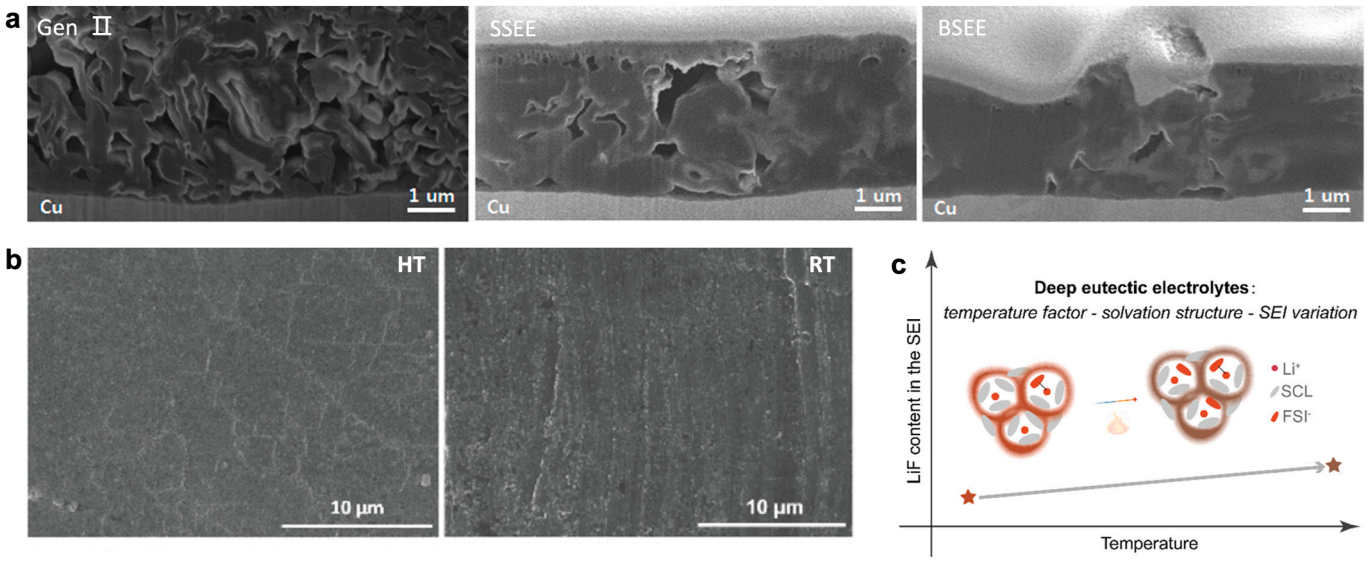

Fig. 6. (a) Cryo-FIB cross-sectional SEM images of the Li morphology after the first cycle for Gen II, SSEE, and BSEE [41] (Reproduced from Ref. 41 with permission from American Chemical Society); (b) SEM images of Li plating in a Li/Li cell operating at high temperatures and at room temperature; (c) the relationship between temperature and the components of a SEI [9] (Reproduced from Ref. 9 with permission from American Chemical Society).

exhibits branches and voids. The porosity of plated Li decreased in SSEE and BSEE but without the formation of dendritic Li.

Operating temperature also influences the properties of the SEI and the solvation structure. As reported by Hou et al., high temperatures promote coordination between Li ions and anions (FSI^-), thus increasing the number of anions in the solvation shell, which fosters a LiF-rich SEI with high ionic conductivity. The compact and stable SEI facilitates dense, smooth Li plating (Figs. 6b and c) [9].

The chemical composition and mechanical properties of the SEI largely determine the Li plating/stripping behavior. The electrochemical process also affects LMB performance by controlling the SEI's properties. Given the various lowest unoccupied molecular orbital (LUMO) of Li salts and solvents, it is feasible to manipulate the SEI composition by controlling electrolyte decomposition. A facile potential hold method was proposed by Manthiram et al. to guide more salt-derived SEIs [42]. The decomposition potential of ethyl methyl carbonate (EMC), 1,2-dimethoxyethane (DME), LiDFOB, lithium bis(fluorosulfonyl)imide (LiFSI), and lithium bis(trifluoromethanesulfonyl)imide (LiTFSI) was elucidated by cathodic linear sweep voltammetry (LSV), yielding values of 0.3, 0.8, 1.86, 1.12, and 1.33 V, respectively. Based on the specific decomposition potential of different components, holding the potential at 0.1 V ensures the decomposition of both solvents and salt, and holding it at 1.3 V reduces the solvent reduction. The XPS results for the decomposition products on Cu foil (1 M FSI in DME as electrolyte) after 18 h of holding the potential at 0.1 and 1.3 V validate the hypothesis that the SEI can be configured using the potential hold method. The higher intensity of LiF (LiFSI salt decomposition product) when a 1.3 V potential hold was applied and the reduced intensity of C–O/C–C originated from organic solvent decomposition, which was observed. As a result, the CE of the Li//Cu cell increases to 99.14% after 18 h of potential hold at 1.3 V, compared to the without potential hold (98.27%).

In summary, as shown in Fig. 7, the properties of the SEI largely determine the Li plating performance. High ionic conductivity, electronic insulation, and sufficient mechanical strength are significant factors for achieving uniform Li plating beneath the SEI. The high ionic conductivity provides even ionic flux, avoiding localized hot spots for dendritic Li growth. The low electric conductivity eliminates localized high currents and prevents continuous side reactions between the Li metal and electrolyte. A robust and dense SEI with a Young's modulus of 4.0 GPa and an elastic modulus of 3.0 GPa suppresses Li dendrite eruption through the SEI and renders a smooth, uniform Li plating by providing uniform stress distribution, which is the prerequisite for high Coulombic efficiency [40]. Artificial SEI and electrolyte engineering are effective strategies to improve the SEI's properties by manipulating its composition, conductivity, and mechanical strength. Furthermore, as SEI properties are largely dependent on the electrolyte's configuration, (localized) high-concentration electrolytes and additives are widely used to manipulate the Li-ion solvation structure and SEI formation. For example, a salt-derived SEI that is rich in LiF and has high mechanical strength, ionic conductivity, and electrochemical stability facilitates uniform Li plating and stable cycling in LMBs. Using a specific potential hold during the LMB's first cycle, a salt-dominated SEI can be derived due to the different decomposition potentials of the salt and solvents.

4. Electro-chemo-mechanical Li plating in solid-state electrolytes

Lithium metal solid-state batteries (LMSSBs) offer improved energy density and safety by replacing the flammable liquid electrolyte with a solid-state electrolyte (SSE) [41,42]. However, their performance is largely determined by the lithium/SSE interface and its dynamic evolution during cycling. When the liquid electrolyte is replaced by a SSE, the mechanical characteristics of the solid–solid interface result in a complex set of electro-chemo-mechanically coupled interfacial degradation phenomena (Fig. 8) [43–45].

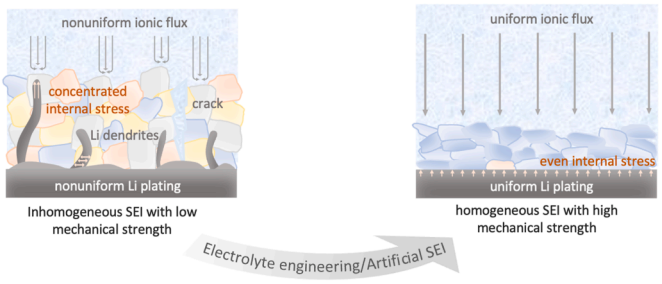

Fig. 7. A schematic of the electro-chemo-mechanical function of the SEI on a Li metal anode.

4.1. General electro-chemo-mechanical considerations

For a SSB, maintaining intimate contact at the interface while accommodating structural and morphological changes associated with lithium plating/stripping is difficult due to the lack of electrolyte wettability. Poor interfacial contact and (electro)chemical side reactions between the lithium metal and the SSE may result in interfacial heterogeneities, where different phases of the interface exhibit varying electrochemical and mechanical properties. These electro-chemo-mechanical heterogeneities affect ion transport by altering the electrical and stress fields at the interface, hence directly influencing the lithium electrodeposition stability [46–49]. Monroe and Newman studied the role of electrochemical-mechanical coupling [50,51]. Their findings predicted that a SSE with roughly twice the shear modulus of lithium ($G_{Li} > 6$ GPa) could mechanically suppress dendrite growth. However, despite the use of a SSE with a shear modulus higher than that of Li, dendrites have been observed to mechanically penetrate through the bulk of the solid electrolyte and short-circuit the cell [52–54], proving that a deeper understanding of the role of mechanics in dictating reaction kinetics is needed. In actuality, the mechanical stresses significantly affect the free energy landscape of the redox reactions at the interface, which can be correlated to changes in the

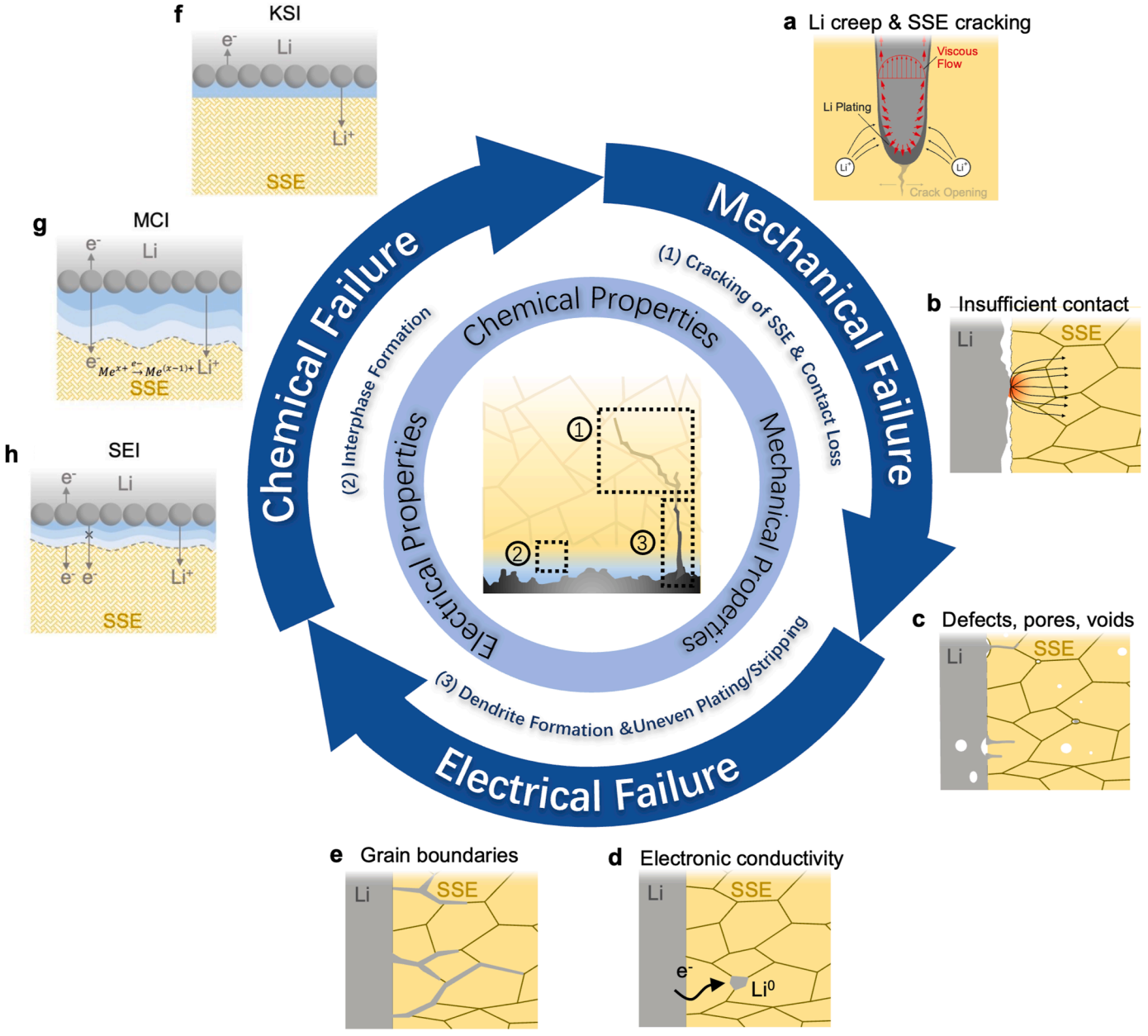

Fig. 8. Schematic representation of the relationship between electro-chemo-mechanical processes and failure modes in LMSSBs, such as dendrite formation and growth, mechanical degradation (SSE cracking and void formation), as well as (electro)chemical interphase formation. (a–d) Illustrate different types of interfaces resulting in chemo-electro-mechanical degradation. Image (a) zooms in on a Li filament where stress accumulates at the tip, causing SSE cracking and Li creep. Li dendrites in the SSE are attributed to: (b) insufficient interfacial contact causing current constrictions; (c) pre-existing defects, pores, or voids where Li can penetrate, forming a filament; (d) electronic conductivity of the SSE; and (e) grain boundaries [61]. (Reproduced from Ref. 61 with open access from the Electrochemical Society); (f–h) schematic of the three different types of interfaces between Li metal and a SSE; (f) a kinetically stable interface (KSI); (g) a mixed conducting interphase (MCI); and (h) a solid electrolyte interphase (SEI) [67].

equilibrium potential and exchange current density [49]. Electrodeposition stability is also affected by the partial molar volume ratio and stress-driven transport, where a combination of high (low) lithium molar volume and high (low) shear modulus is required [55]. Fundamentally, the mechanical characteristics and microstructural heterogeneity of the SSE/lithium metal interface lead to a distinct set of electro-chemo-mechanical processes, culminating in various degradation and failure mechanisms (Fig. 8).

4.2. Effect of interface morphology

It is important to investigate the effects of the interplay between intrinsic (interface morphology, molar volume ratio) and extrinsic (stack pressure, temperature, current density) factors on the electro-chemo-mechanical instability of the lithium metal/SSE interface [49]. The rigid nature of the interface makes it difficult to retain contact during lithium metal stripping, so voids form at the interface [56]. In the absence of stack pressure, void formation is influenced by the interplay between lithium vacancy diffusion and lithium anodic dissolution. If the dissolution rate exceeds the vacancy diffusion rate, voids can form by an accumulation of vacancies at the interface. The introduction of new heterogeneities at the interface alters the electric and stress field distribution, further promoting unstable electrodeposition. The plastic deformation of lithium metal by applying stack pressure can help to replenish voids and retain contact at the interface [57]. Therefore, moderate stack pressure is often needed to maintain intimate interfacial contact during cycling. However, too high of a stack pressure could mechanically short-circuit the cell as the low yield strength of lithium allows it to creep through micropores in the SSE [58,59].

4.3. Lithium dendrite formation and growth

Unstable electrodeposition and lithium dendrite growth can be influenced by multiple factors, and the propagation can be described by different growth modes. Similar to voids, all interfacial defects, such as cracks and chemical inhomogeneities, alter lithium plating/stripping, causing mechanical and electrical hotspots. As Li metal preferentially accumulates in these interfacial flaws, stress builds up in the enclosed regions, causing the SSE to fracture [54,60,61]. Once cracks have formed, the application of stack pressure or continuous deposition can cause localized lithium metal creep, further propagating both the crack and dendritic growth within it. Dendrites thus propagate due to plating-induced fracturing of the SSE, and an increase in stack pressure increases the risk for dendrite-induced short-circuiting. However, mechanical stresses can also be used to deflect the dendrite trajectory [59]. A study by Hu et al. demonstrated how dendrite growth could be inhibited by deflecting SSE-induced fractures by using a multi-layered SSE with dissimilar elastic moduli [62]. Modification of the bulk SSE properties is therefore an additional mitigation strategy. One study showed that electrolyte densification from 83% to 99 % could increase the critical plating current density for dendrite formation from 1 to 10 mA cm^{-2} [58].

Dendritic growth is not attributable solely to the microstructure of the SSE and interface. Another observed dendrite growth mode is through the SSE grain boundaries, due to their inherently different ionic conductivity and mechanical properties compared to the bulk [52–54]. An additional characteristic of LMSSBs is that Li can be observed to nucleate within the bulk SSE, due to electronic conductivity [63–65]. Seemingly, the conductivity and the lithium-ion transport mechanism have a significant effect on the lithium plating/stripping process and hence the lithium dendritic growth mode [66]. At a microscopic scale, lithium-ion transport is influenced by atomic-level interactions (lattice dynamics, diffusion pathways, etc.). At a mesoscopic level, it shifts towards factors influencing the transport at interfaces (grain boundaries, contact points). On the bulk level, the transportation properties are influenced by factors such as electrolyte thickness, porosity, and mechanical stability. Various strategies are needed to optimize SSE design, which can be achieved by bringing a multiscale perspective to its ion transport mechanisms.

4.4. Interphase formation

Most SSEs are not (electro)chemically stable against Li metal. Electrolyte reduction typically occurs at the Li metal/SSE interface to form an interphase due to the accumulation of decomposition products. In general, the Li metal/SSE interface can be classified into one of three types, schematically presented in Figs. 8a–c [67], which can be distinguished based on their electronic and ionic properties [68]: (a) a non-reactive and thermodynamically stable interface, where no interphase is formed; (b) a reactive and mixed conducting interphase (MCI), where simultaneous electronic and ionic conductivity leads to continuous degradation of the interface; and (c) a reactive but meta-stable interphase, ionically conductive but electrically insulating, hence preventing further parasitic reactions and limiting the growth of the interphase to form a "stable SEI." Although a relatively stable interphase might form, the cycling performance might still be affected by the ionic conductivity of the interphase, as it influences the redox reaction kinetics of the interface. These interphase formation behaviors — i.e., elemental and structural interfacial evolution — can impact the electro-chemo-mechanical behavior of the SSB. Interphase formation results in volume changes, which can induce local expansions or contracts. By investigating the evolution of stack pressure for different electrolytes, a pressure relaxation attributed to a volume reduction in the SSB was observed for a cell chemistry exhibiting continuous interphase growth, in contrast to one that formed a passivating interphase [69]. In another study, expansion of the SSE itself was observed for a third cell chemistry, which caused in-plane stress evolution and fracturing of the SSE [73]. Such added mechanical stress can further alter the thermodynamics and energy landscape of the interface, affecting both (electro)chemical reactions and diffusion kinetics [52], which highlights the strong correlation between the electro-chemo-mechanical instability of the interface and various degradation phenomena.

4.5. Strategies to bypass interfacial instability

Fig. 8 highlights the intimately linked and coupled electro-chemo-mechanical properties, processes, and failure modes in LMSSBs. Various efforts have been made to counteract the elemental and morphological problems associated with lithium metal anodes and SSEs using clever structural designs or chemical modifications of the interface and bulk materials [44]. Metal and metalloid interlayers that form a lithium metal alloy are widely used to improve the plating/stripping performance of the lithium/SSE interface [61]. Other types of interlayers, including a sacrificial interlayer aimed at forming an artificial "SEI" line ionically conducting interphase, have been used to mitigate further reductive decomposition of the SSE and, in certain cases, improve the morphological stability of the interface [2,70–73]. However, the addition of an interlayer generates two new interfaces: towards (i) the current collector or lithium metal/interlayer and (ii) the interlayer/SSE. These additional interfaces will have their own electro-chemo-mechanical properties, adding further complexity and requiring additional research. Further work is needed to ensure the safe and long-term operation of LMSSBs, but understanding and probing the electro-chemo-mechanical phenomena in LMSSBs will require advanced multiscale, *in situ*, and *operando* characterization techniques.

5. Methodology for understanding electro-chemo-mechanics

5.1. Imaging characterization methods

Recently, research on the mechanisms of the Li plating/stripping processes has been promoted by the implementation of electron

microscopy and X-ray imaging methods, which can visualize the evolution of the morphology, structure, and physicochemical properties of Li and the SEI [74,75] from the atomic to the macroscopic scale (Fig. 9a). One important microscopic instrument that provides information about the structural and chemical composition in bulk at the atomic level is transmission electron microscopy (TEM) [76,77]. *In situ* TEM can provide direct visualization of Li plating and SEI formation with atomic-scale resolution, and elemental distributions as well as binding energies can be obtained by combining TEM with selected area electron diffraction (SAED) and electron energy-loss spectroscopy (EELS) [78,79]. At the nanoscale, scanning electron microscopy (SEM) has been used to determine the morphology of plated Li. Notten et al. observed moss-like Li and dendrite-like Li using *in situ* SEM [80,81]. Rong et al. developed *in situ* electrochemical SEM (EC-SEM) to study Li plating/stripping in an ether-based electrolyte with two different additives. Their work revealed that the additives affected the lithium dendrite growth speed and mechanism [82]. Recently, Cui et al. demonstrated an *in situ* SEM technique, externally coupled with electrochemical testing, to monitor the dynamics of Li plating on 10 metallic substrates for all-solid-state batteries with LAGP as the SSE. They found various Li morphologies, a dendrite-like morphology, and an in-plane particulate-like pattern, as well as different modes of alloying between Li and certain substrates before Li growth [83]. However, the Li surface inevitably is damaged by high-energy electron-beam irradiation, which leads to the decomposition of organic electrolytes during *in situ* SEM and TEM experiments [84,85]. Cryo-scanning transmission electron microscopy (cryo-STEM) and cryo-FIB are thus being utilized to preserve the original states of materials and interfaces, facilitating high-resolution imaging [86,87].

In addition to 2D imaging techniques, XTM is an effective strategy to investigate the 3D morphological evolution of Li at the microstructural level [88]. During XTM measurements, projections are taken of a rotating sample at various angles, and the resulting 2D images are reconstructed into a 3D volume, as shown in Fig. 10a [89]. This method facilitates qualitative assessments, such as defect visualization and the monitoring of changes in electrode morphology. Through segmentation, it also yields quantitative data, including volume fraction, surface area, and tortuosity [90]. As a result, XTM gives both macroscopic and microscopic information about the morphology of plated Li during battery operation.

Both laboratory-based and synchrotron-based XTM have been utilized to investigate processes occurring at the Li metal anode [91]. Compared to other techniques, XTM coupled with high-flux synchrotron X-rays enables *in situ* and operando measurements. This capability is attributed to high temporal and spatial resolutions that enable the capture of dynamic processes within a battery cell [91]. For instance, Eastwood et al. utilized synchrotron-based X-ray phase-contrast tomography in a separator-less symmetrical Li cell to differentiate mossy Li from high surface area Li salt formations. This distinction relied on the structures' different X-ray attenuation [92]. Sadd et al. confirmed the presence of mossy Li in a Li/Cu cell. Their 3D visualization of plated Li allowed differentiation between needle-like and mossy structures (Fig. 10b). Additionally, the study identified Li metal microstructures distributed as islands post-plating [7].

To replicate real battery cell conditions, Sun et al. employed in-line phase-contrast X-ray tomography to investigate the evolution of Li microstructures within symmetrical Li cells with a Celgard 2325 separator. Their findings revealed continuous dissolution of the bulk Li anode

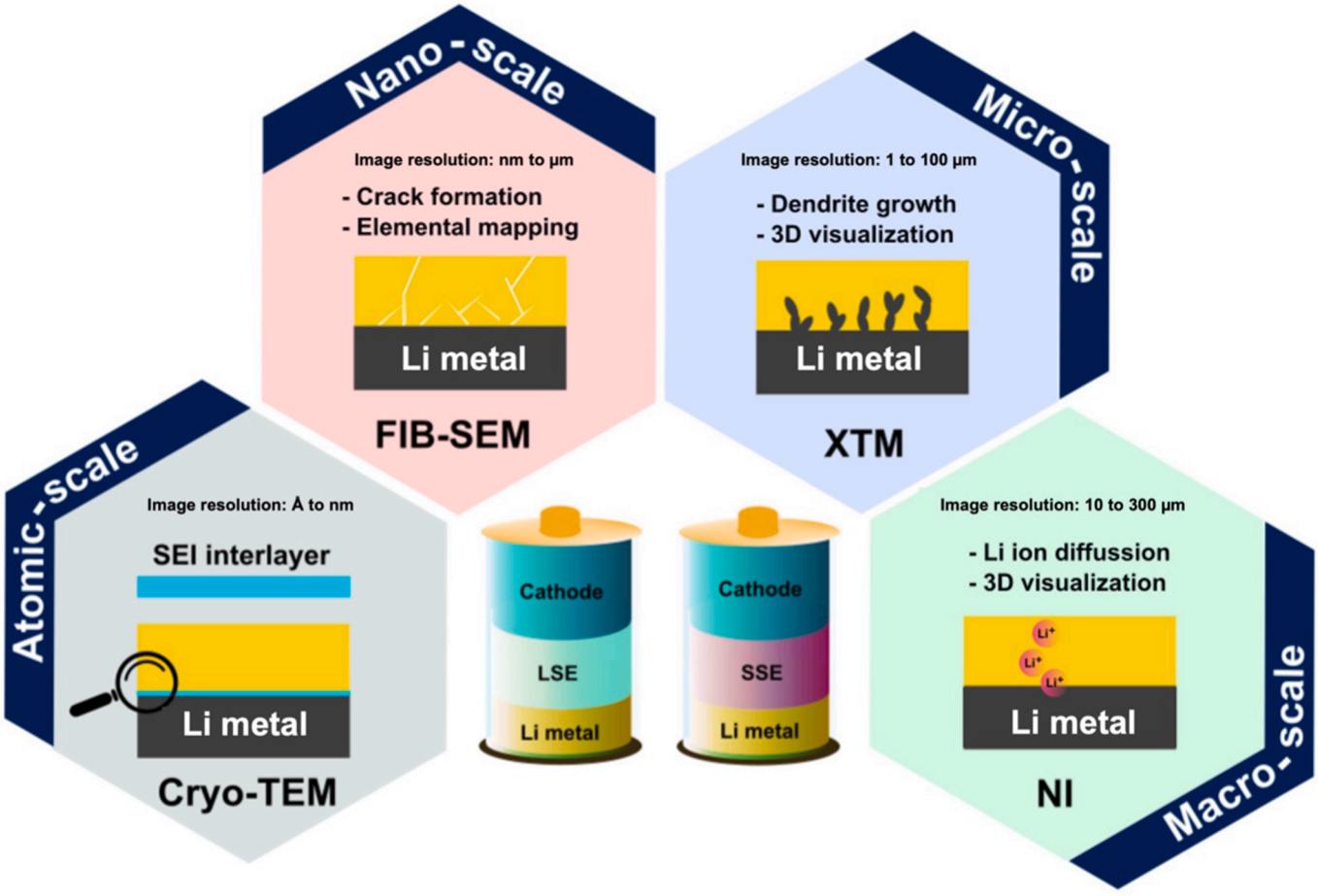

Fig. 9. Illustration of various imaging techniques and their image resolution and function, from atomic to macroscopic levels.

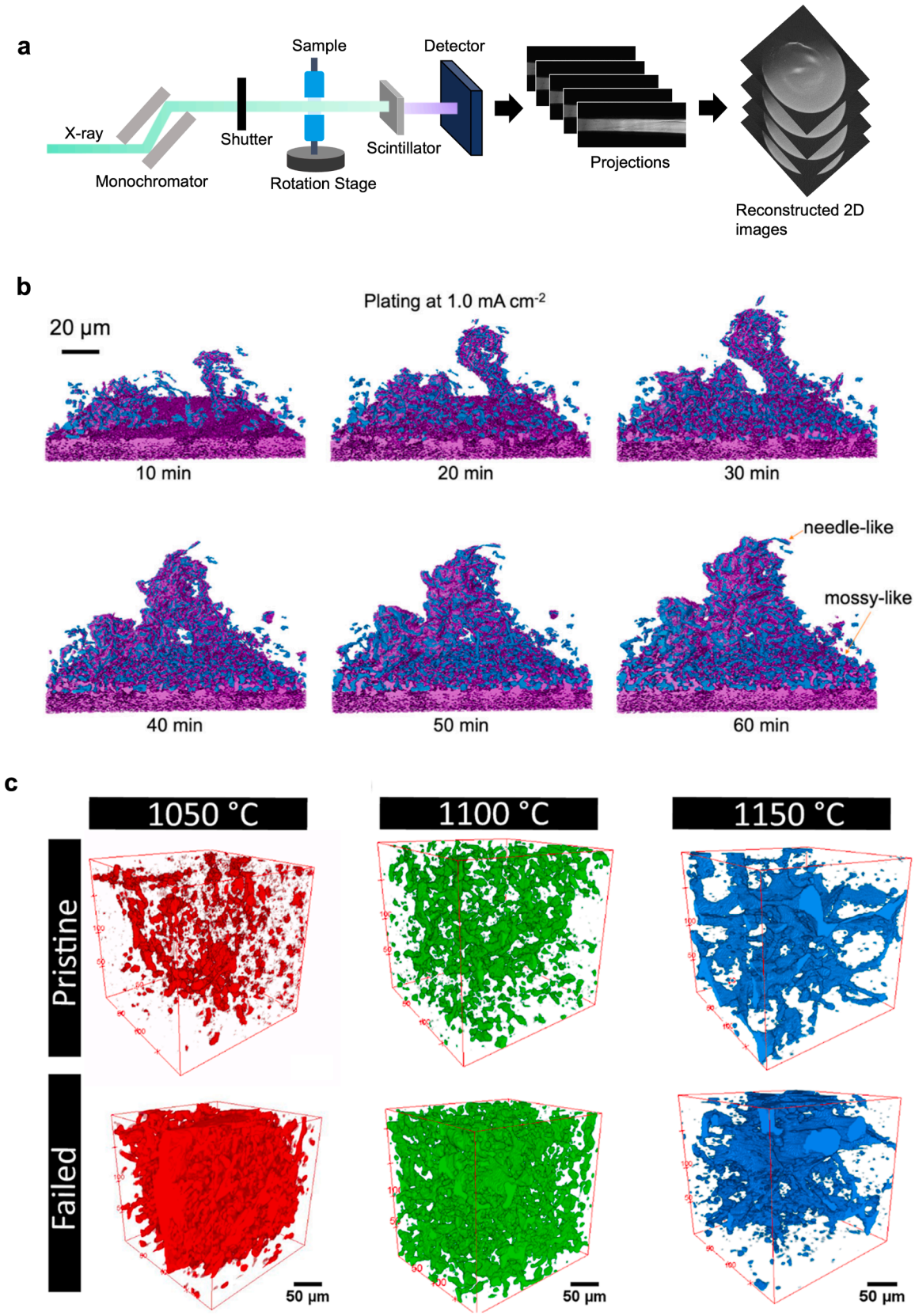

Fig. 10. (a) Illustration of X-ray tomography experimental setup [89] (Reproduced from Ref. 89 with permission from American Chemical Society); (b) 3D rendering of Li microstructures at different plating times [7]; (c) 3D volumes of void phase in LLZO electrolyte prepared at different temperatures [95] (Reproduced from Ref. 95 with permission from American Chemical Society).

during each stripping step, leading to the formation of cavities. Subsequent plating resulted in the accumulation of significant quantities of Li microstructures, forming a porous lithium interface (PLI) that occupied voids generated from the previous dissolution [93]. Taiwo et al. confirmed the presence of voids on the Li metal electrode surfaces within a graphite/glass fiber separator/Li half-cell employing synchrotron and laboratory-based X-ray micro-tomography. They observed pits forming on the electrode surface, which gradually increased in diameter and depth during discharge, due to Li dissolution. This study highlights the critical role of separator morphology in managing or preventing dendrite growth, especially in high tortuosity separators, emphasizing the urgent need for separator design [94].

The application of tomography techniques can be particularly helpful for investigating SSEs. For instance, Shen et al. utilized *ex situ* synchrotron XTM to study structural changes of a garnet-type ($Li_7La_3Zr_2O_{12}$, LLZO) SSE after cell failure, as shown in Fig. 10c. They found that Li plating increases with pore size distribution, suggesting that metallic Li can be plated in isolated forms or accumulate within pores. They concluded that porosity decreases with temperature, and SSEs with connected pore regions promote dendrite formation at a lower critical current density [95]. Dixit et al. used *in situ* synchrotron tomography to track morphological transformations in Li metal electrodes in Li|LLZO|Li cells. They developed advanced image processing and machine learning methods to process low-contrast images for quantitative analysis. They suggested that factors such as high mass flux at the interface, inadequate metal diffusion, and creep flow contribute to void generation, concluding that high porosity at the interface indicated void formation and interfacial delamination [96]. Voids have also been observed in other SSEs. Lewis et al. found both voids and interphases between $Li_{10}SnP_2S_{12}$ (LSPS) and the Li electrode, which grew substantially after stripping. These voids formed when Li ions were removed faster than the Li metal could be replaced. They suggested that cell failure arises from loss of contact at the stripping interface [97].

While X-ray techniques provide crucial insights into electrode alterations involving heavier elements, their low sensitivity renders them inadequate for analyzing lithium and light-element electrolytes [98]. Increasingly, neutron imaging (NI) is being used for battery characterization. Neutrons are electrically neutral and interact with atomic nuclei via short-range strong nuclear forces while remaining unaffected by electrons, enabling structural characteristics to be probed from the surface to the interior, even under extreme conditions [99]. For instance, Bradbury et al. used *in situ* neutron tomography to visualize Li-ion transport through a SE separator [100].

The unique nuclear scattering properties of neutrons also make them highly sensitive to light elements. The isotope-dependent nature of neutron scattering results in distinct scattering lengths for different isotopes, allowing for their differentiation. Moreover, with a magnetic moment of −1.913, neutrons can interact with unpaired electrons in magnetic materials through dipole–dipole interactions, making them a valuable tool for studying magnetic structures and fluctuations. The characteristics of neutrons point toward their potential application to characterize lithium batteries. Neutron diffraction (ND) [101] fills the gaps in crystallographic information that X-ray diffraction cannot provide and thus has been utilized to investigate the evolution of lattice parameters, the atomic occupancy of Li/O, and chemical bonding in inorganic SSEs. Through this analysis, along with structural studies of doped electrolytes, the Li-ion transport mechanism in these materials has been elucidated. Small-angle neutron scattering (SANS) [102] is a useful method for analyzing the shape, structure, and distribution of particles or aggregates dispersed in a continuous medium over time. The inhomogeneity of inorganic SSEs at specific spatial scales can be investigated by SANS, including the occurrence of abnormal grains and Li dendrites. In addition, neutron imaging techniques enable the direct observation of Li metal plating/stripping, electrolyte consumption, and gas evolution due to the high visibility of light-Z elements, especially for hydrogen and lithium.

In situ nuclear magnetic resonance (NMR) spectroscopy is used to quantitatively analyze Li plating owing to the high sensitivity of ^{7}Li NMR. *In situ* magnetic resonance imaging (MRI) is a noninvasive tool to both probe Li microstructure and provide quantitative data.

5.2. Computational techniques

Battery system design and comprehension require the use of modeling and simulation. These are particularly valuable when experimental data are insufficient to explain underlying mechanisms or are difficult or costly to obtain, or when the parameter space is too vast for efficient optimization through experiments alone [103]. In addition, the use of computations and experiments together can hasten advancements in battery science and technology [104].

Multi-physics field modeling is an effective tool for understanding the process of Li plating and the influences of various factors. The approach uses a number of basic laws and equations, solved simultaneously, to reveal the interplay between the physical and chemical attributes of the system being investigated [105,106], providing direction for focused battery optimization [107]. Phase-field modeling (PFM) is used to simulate the interface evolution between two different materials and to model the microstructural evolution of dendrites in lithium metal batteries [108]. Finite element modeling (FEM) uses numerical models in which the partial differential equations describing the model are solved by discretizing a continuous system into a finite number of elements [106].

Some work on modeling based on the finite element technique to understand the electro-chemo-mechanics of Li plating has been reported [109,110]. This technique has been extensively used in structural mechanics and stress computation [110]. In brief, this approach provides an approximation of the physical system under study [109] while solving differential equations based on a number of various concepts [110]. For instance, Zhang's group presented a quantitative electrochemical–mechanical model based on the finite element method by coupling multi-physics, including current distribution, mass transport, electrochemical reactions, and stress distribution [12]. Their findings revealed that structural uniformity can lead to SEI stability. They also recommended that having a SEI with a 3.0 GPa elastic modulus is preferable to having one with high mechanical strength [12]. This method broadens the understanding of Li plating from the experimental perspective. In addition, Xiong et al. carried out a series of studies using electro-chemo-mechanical modeling and the visualization of stress fields to examine SSE failure mechanisms rooted in defects and Li filament growth [111–113]. They created an electro-chemo-mechanical model to study the characteristics of an artificial SEI in order to achieve uniform Li electrodeposition, concluding that stress concentration and preferential deposition of Li can be mitigated by increasing the SEI's ionic conductivity over a critical level. Elsewhere, Matic's group investigated Li plating by building a phase-field model based on the effects of an artificial SEI [8], various metal substrates [14], and exchange current density [16].

In summary, multiscale characterization enables the gathering of diverse information to better understand the electro-chemo-mechanics of the Li metal anode. Experimentation takes time, but it is the foundation for multiscale modeling. Recent advancements in computational approaches can aid in experimental characterization and explain phenomena that occur at the atomic level.

6. Conclusion and outlook

LMB performance is highly dependent on the Li plating/stripping behavior, which is an electro-chemo-mechanically coupled process. This review has summarized the Li plating process in liquid-state electrolyte systems and solid-state electrolyte systems, and the function of the SEI from this perspective. We have also systematically discussed the methodology for investigating Li plating/stripping and SEI properties.

During Li plating, Li ions de-solvate at the interface and adsorb on the surface of the substrate, and early nucleation takes place, accompanied by charge transfer and the reduction of Li ions to metallic Li. Thus, the morphology of plated Li is related to the substrate's properties, including its lithiophilicity and mechanical strength. A higher binding energy and a lower surface energy give the substrate stronger lithiophilicity, resulting in a lower nucleation overpotential, which contributes to a uniform and dense Li plating morphology. The Li growth process is also affected by the current density, overpotential, temperature, and pressure. The factors for achieving uniform, dense Li plating are summarized as follows. In a liquid-state electrolyte: 1) high lithiophilicity of the substrate leads to low nucleation overpotential; 2) a low self-diffusion barrier renders larger Li nuclei and Li substructures with a lower aspect ratio, resulting in more uniform Li plating; 3) low current densities inhibit dendritic Li formation by reducing current hot spots at the tip of the plated Li and mitigating the formation of branched Li substructures; 4) low overpotential leads to Li nuclei with a larger radius, rendering uniform, dense Li plating; 5) low exchange current densities facilitate uniform, dense Li plating with larger-radius Li nuclei, which suppresses the growth of Li dendrites and contributes to high Coulombic efficiency; 6) a sufficient external pressure of about 14 MPa prevents tip growth in favor of lateral growth. The current density limit (J_{lim}) for uniform Li plating is calculated based on Sand's time theory. When the current density $J < J_{lim}L$ in a finite-L system, no tip-grown dendrites occur. An electrolyte with a high salt concentration and a low anion transference number is desirable for achieving a longer Sand's time and suppressing Li plating instabilities.

Researchers now have a systematic understanding of the electro-chemo-mechanics of a Li metal anode in LSEs, but limitations remain: 1) the Li plating and stripping processes are influenced by multiple factors in what is a highly coupled system, and it is difficult to clarify the mechanism of a specific isolated parameter. For example, changing the current density alters the reaction dynamics of Li-ion diffusion and charge transfer simultaneously, further affecting the electric field distribution and interphase formation. Hence, it is hard to analyze the influence of current density alone on Li plating/stripping behaviors; 2) experimental research should be combined with theoretical studies to build a solid and in-depth understanding of the mechanisms of Li metal anodes; 3) the transition from lab-scale research to practical applications has not been studied, and the feasibility of up-scaling remains uncertain. Studies should be carried out in multiple directions, including experience, theory, aspect, and up-scaling, to achieve LMBs for practical applications.

The SEI plays an important role in the Li plating/stripping processes. Li ions de-solvate at the interface and are transported through the SEI, then are reduced to metallic Li beneath the SEI, accompanied by Li nucleation and early growth. Therefore, the ionic/electric conductivities, mechanical properties, physicochemical properties, and morphological structure of the SEI largely determine the nature of Li plating. The character of a SEI can be tuned by electrolyte engineering, since the SEI is a passivation layer induced by the reactions between the electrolyte and the Li metal anode. SEI composition can also be regulated by specific electrochemical potential hold, which facilitates a salt-derived SEI by holding the potential at a level lower than that of anion reduction and higher than that of solvent decomposition. The factors for an ideal SEI are as follows: 1) a SEI with a Young's modulus of 4.0 GPa and an elastic modulus of 3.0 GPa can accommodate volume expansion and avoid cracking during plating, thus suppressing Li dendrite eruption through the SEI and yielding smooth, uniform Li plating by ensuring uniform stress distribution; 2) a high inorganic content in the SEI (for example, a LiF-rich SEI) gives it robustness as well as higher ionic conductivity and mechanical strength, mitigating stress concentration after Li plating; 3) a low electronic conductivity inhibits current hot spots that would otherwise lead to dendritic Li growth; 4) a high ionic conductivity facilitates fast ion transport, resulting in uniform Li plating; 5) a uniform SEI yields homogenous ionic/electronic conductivities, avoiding the concentration of ions/current in hot spots; and 6) a thin, compact morphology helps eliminate continuous side reactions between the electrolyte and the Li electrode.

Although an in-depth understanding of the electro-chemo-mechanics of SEIs has been established, the field remains attractive but largely unexplored, for various reasons: 1) Despite decades of research, a universally accepted model describing SEI formation, evolution, and degradation under real battery conditions is still lacking. Existing models often oversimplify SEI chemistry and fail to account for dynamic changes that occur during long-term cycling. A multi-scale understanding of the SEI formation mechanism and properties is essential. 2) Most SEI studies rely on ex situ characterization, which does not capture the real-time evolution of a SEI. *In situ* and operando techniques, such as *in situ* TEM and *in situ* XPS, are essential for observing SEI formation and evolution to understand SEI dynamics. However, these methods are still in their infancy and require further refinement for widespread application. 3) SEI modification strategies, such as electrolyte additives, artificial SEI coatings, and advanced electrolyte formulations, have shown promise in laboratory settings. However, scaling up these approaches for commercial battery systems while maintaining cost-effectiveness and long-term stability remains a challenge. 4) The commonly accepted understanding of SEI structure is oversimplified and far different from the actual situation. For example, the SEI is considered an "inner inorganic, outer organic" structure, whereas in practice, it is an inorganic–organic braided structure because the reductions of solvent and salt occur almost simultaneously. In addition, unstable components in the SEI are oxidized during charging, causing it to evolve, which makes the breathable and transformational structure of a SEI difficult to characterize and track.

Understanding and controlling the solid-state electrolyte/lithium metal anode interface is one of the major hurdles for solid-state batteries. Both the chemical and morphological evolution as well as the mechanical characteristics contribute to the interface stability. Defects at the interface and in the SSE, such as voids, impurities, phase distributions, cracks, grain boundaries, and porosity, can alter the stress field and cause a non-uniform distribution of the electric field, promoting dendritic growth and plating-induced fracture of the SSE. Furthermore, certain SSEs are (electro)chemically unstable against Li metal and form a resistive interphase. Advanced SSEs with mechanical robustness, high (electro)chemical stability, and low electronic but high ionic conductivity are needed to ensure stable, high-performing SSBs not only at room temperature but also at low stack pressure. Using high stack pressures and temperatures to enhance performance is a rather simple strategy, but as these variables change, new mechanisms may influence the interfacial electro-chemo-mechanics. In the interest of practical applications, a focus on the effects of low stack pressures (< 1 MPa) and other practically relevant testing conditions on interfacial evolution is urgently required. An alternative attractive SSB architecture is the "anode-free" configuration. Manufacturing SSBs with lithium metal anodes requires highly controlled atmospheres, making large-scale implementation expensive and challenging. Opting for a SSB with zero excess lithium offers a potential solution, with simulations enabling even higher energy density. As in lithium-excess SSBs, the stable operation of anode-free SSBs is largely determined by the interfacial and material evolution. However, the lack of a lithium reservoir makes them sensitive and susceptible to new complex electro-chemo-mechanically coupled processes. Further research is needed to fully understand how the behavior of anode-free SSBs differs from that of conventional excess-lithium SSBs.

As the SSB field continues to grow, there is a need for systematic reporting of testing conditions. The conditions vary widely across literature, often with little information being provided about the fabrication of the SSB cell. Yet, the assembly methodology directly influences interface quality and thus cell performance. All assembly steps must be considered, making it advisable to report all procedural details, from material processing to cleaning. Future strategies may focus on

engineering interfaces by designing SSE properties and implementing interlayers. Further attention is needed on the characterization of interphase growth in SSBs and its long-term influence on cell performance. Advanced *in situ*/operando characterization techniques are needed to improve our understanding of SSB operation and degradation and thereby further the development of this technology.

Last but not least, diverse characterization approaches from the atomic to the particle level complement one another and provide better insights into future battery advancements. For example, XTM can analyze electrode morphological changes during Li plating/stripping at better spatial and temporal resolutions. Li-ion migration during the plating/stripping process is easily detectable when used in conjunction with neutron imaging. Although the NI method is limited by the number of facilities accessible around the world, its sensitivity for analyzing Li-ion mobility makes it an appealing approach that will increasingly be part of the battery characterization toolbox. Furthermore, combining NI and XTM imaging, as well as computational modeling, helps to strengthen our grasp of the relationship between materials from the macroscopic to the atomic level.

CRediT authorship contribution statement

Quan Wu: Writing – original draft, Visualization, Validation. **Elin Dufvenius Esping:** Visualization, Investigation. **Marita Afiandika:** Writing – original draft, Visualization. **Shizhao Xiong:** Writing – review & editing, Writing – original draft, Supervision. **Aleksandar Matic:** Writing – review & editing, Writing – original draft, Supervision.

Competing financial interests

The authors declare no competing financial interests.

Declaration of competing interest

The authors declare that they have no known competing financial interests or personal relationships that could have appeared to influence the work reported in this paper.

Acknowledgments

This project has received funding from The Swedish Electricity Storage and Balancing Centre, The Swedish Energy Agency and Wallenberg Wood Science Center. The work was financially supported by the National Natural Science Foundation of China (22479067).

References

[1] W. Cao, Q. Li, X. Yu, H. Li, Controlling Li deposition below the interface, eScience 2 (2022) 47–78.
[2] S. Zhang, S. Li, Y. Lu, Designing safer lithium-based batteries with nonflammable electrolytes: a review, eScience 1 (2021) 163–177.
[3] S. Li, M. Jiang, Y. Xie, H. Xu, J. Jia, J. Li, Developing high-performance lithium metal anode in liquid electrolytes: challenges and progress, Adv. Mater. 30 (2018) 1706375.
[4] K.G. Naik, B.S. Vishnugopi, J. Datta, D. Datta, P.P. Mukherjee, Electro-chemo-mechanical challenges and perspective in lithium metal batteries, Appl. Mech. Rev. 75 (2023) 010802.
[5] Y. Xu, K. Dong, Y. Jie, P. Adelhelm, Y. Chen, L. Xu, P. Yu, J. Kim, Z. Kochovski, Z. Yu, W. Li, J. LeBeau, Y. Shao-Horn, R. Cao, S. Jiao, T. Cheng, I. Manke, Y. Lu, Promoting mechanistic understanding of lithium deposition and solid-electrolyte interphase (SEI) formation using advanced characterization and simulation methods: recent progress, limitations, and future perspectives, Adv. Energy Mater. 12 (2022) 2200398.
[6] X.-R. Chen, B.-C. Zhao, C. Yan, Q. Zhang, Review on Li deposition in working batteries: from nucleation to early growth, Adv. Mater. 33 (2021) 2004128.
[7] M. Sadd, S. Xiong, J.R. Bowen, F. Marone, A. Matic, Investigating microstructure evolution of lithium metal during plating and stripping via operando X-ray tomographic microscopy, Nat. Commun. 14 (2023) 854.
[8] Y. Liu, X. Xu, O.O. Kapitanova, P.V. Evdokimov, Z. Song, A. Matic, S. Xiong, Electro-chemo-mechanical modeling of artificial solid electrolyte interphase to enable uniform electrodeposition of lithium metal anodes, Adv. Energy Mater. 12 (2022) 2103589.
[9] Q. Hou, P. Li, Y. Qi, Y. Wang, M. Huang, C. Shen, H. Xiang, N. Li, K. Xie, Temperature-responsive solvation of deep eutectic electrolyte enabling mesocarbon microbead anode for high-temperature Li-ion batteries, ACS Energy Lett. 8 (2023) 3649–3657.
[10] C. Fang, B. Lu, G. Pawar, M. Zhang, D. Cheng, S. Chen, M. Ceja, J.-M. Doux, H. Musrock, M. Cai, B. Liaw, Y.S. Meng, Pressure-tailored lithium deposition and dissolution in lithium metal batteries, Nat. Energy 6 (2021) 987–994.
[11] Q. Dong, B. Hong, H. Fan, C. Gao, X. Huang, M. Bai, Y. Zhou, Y. Lai, A self-adapting artificial SEI layer enables superdense lithium deposition for high performance lithium anode, Energy Storage Mater. 45 (2022) 1220–1228.
[12] X. Shen, R. Zhang, X. Chen, X.-B. Cheng, X. Li, Q. Zhang, The failure of solid electrolyte interphase on Li metal anode: structural uniformity or mechanical strength? Adv. Energy Mater. 10 (2020) 1903645.
[13] F. Hao, A. Verma, P.P. Mukherjee, Mechanistic insight into dendrite–SEI interactions for lithium metal electrodes, J. Mater. Chem. A 6 (2018) 19664–19671.
[14] X. Jiao, Y. Wang, O.O. Kapitanova, X. Xu, V.S. Volkov, Y. Liu, Z. Song, A. Matic, S. Xiong, Morphology evolution of electrodeposited lithium on metal substrates, Energy Storage Mater. 61 (2023) 102916.
[15] X. Chen, X.-R. Chen, T.-Z. Hou, B.-Q. Li, X.-B. Cheng, R. Zhang, Q. Zhang, Lithiophilicity chemistry of heteroatom-doped carbon to guide uniform lithium nucleation in lithium metal anodes, Sci. Adv. 5 (2019) eaau7728.
[16] Y. Liu, X. Xu, M. Sadd, O.O. Kapitanova, V.A. Krivchenko, J. Ban, J. Wang, X. Jiao, Z. Song, J. Song, S. Xiong, A. Matic, Insight into the critical role of exchange current density on electrodeposition behavior of lithium metal, Adv. Sci. 8 (2021) 2003301.
[17] Y. Lv, Q. Zhang, C. Li, C. Ma, W. Guan, X. Liu, Y. Ding, Bottom-up Li deposition by constructing a multiporous lithiophilic gradient layer on 3d cu foam for stable Li metal anodes, ACS Sustain. Chem. Eng. 10 (2022) 7188–7195.
[18] P. Bai, J. Li, F.R. Brushett, M.Z. Bazant, Transition of lithium growth mechanisms in liquid electrolytes, Energy Environ. Sci. 9 (2016) 3221–3229.
[19] H.J.S. Sand III, On the concentration at the electrodes in a solution, with special reference to the liberation of hydrogen by electrolysis of a mixture of copper sulphate and sulphuric acid, Proc. Phys. Soc. London 17 (1899) 496.
[20] L. Li, S. Basu, Y. Wang, Z. Chen, P. Hundekar, B. Wang, J. Shi, Y. Shi, S. Narayanan, N. Koratkar, Self-heating–induced healing of lithium dendrites, Science 359 (2018) 1513–1516.
[21] X. Yuan, B. Liu, M. Mecklenburg, Y. Li, Ultrafast deposition of faceted lithium polyhedra by outpacing SEI formation, Nature 620 (2023) 86–91.
[22] A. Pei, G. Zheng, F. Shi, Y. Li, Y. Cui, Nanoscale nucleation and growth of electrodeposited lithium metal, Nano Lett. 17 (2017) 1132–1139.
[23] X.-R. Chen, C. Yan, J.-F. Ding, H.-J. Peng, Q. Zhang, New insights into "dead lithium" during stripping in lithium metal batteries, J. Energy Chem. 62 (2021) 289–294.
[24] A.C. Thenuwara, P.P. Shetty, M.T. McDowell, Distinct nanoscale interphases and morphology of lithium metal electrodes operating at low temperatures, Nano Lett. 19 (2019) 8664–8672.
[25] B. Lu, W. Bao, W. Yao, J.-M. Doux, C. Fang, Y.S. Meng, Editors' Choice—methods—pressure control apparatus for lithium metal batteries, J. Electrochem. Soc. 169 (2022) 070537.
[26] X. Shen, R. Zhang, P. Shi, X. Chen, Q. Zhang, How does external pressure shape Li dendrites in Li metal batteries? Adv. Energy Mater. 11 (2021) 2003416.
[27] X. Wang, W. Zeng, L. Hong, W. Xu, H. Yang, F. Wang, H. Duan, M. Tang, H. Jiang, Stress-driven lithium dendrite growth mechanism and dendrite mitigation by electroplating on soft substrates, Nat. Energy 3 (2018) 227–235.
[28] F. Hao, B.S. Vishnugopi, H. Wang, P.P. Mukherjee, Chemomechanical interactions dictate lithium surface diffusion kinetics in the solid electrolyte interphase, Langmuir 38 (2022) 5472–5480.
[29] A. Kushima, K.P. So, C. Su, P. Bai, N. Kuriyama, T. Maebashi, Y. Fujiwara, M. Z. Bazant, J. Li, Liquid cell transmission electron microscopy observation of lithium metal growth and dissolution: root growth, dead lithium and lithium flotsams, Nano Energy 32 (2017) 271–279.
[30] Y. Zhao, M. Amirmaleki, Q. Sun, C. Zhao, A. Codirenzi, L.V. Goncharova, C. Wang, K. Adair, X. Li, X. Yang, F. Zhao, R. Li, T. Filleter, M. Cai, X. Sun, Natural SEI-inspired dual-protective layers via atomic/molecular layer deposition for long-life metallic lithium anode, Matter 1 (2019) 1215–1231.
[31] F. Ding, W. Xu, X. Chen, J. Zhang, M.H. Engelhard, Y. Zhang, B.R. Johnson, J. V. Crum, T.A. Blake, X. Liu, J.-G. Zhang, Effects of carbonate solvents and lithium salts on morphology and coulombic efficiency of lithium electrode, J. Electrochem. Soc. 160 (2013) A1894.
[32] M.S. Park, S.B. Ma, D.J. Lee, D. Im, S.-G. Doo, O. Yamamoto, A highly reversible lithium metal anode, Sci. Rep. 4 (2014) 3815.
[33] X.-Q. Zhang, X. Chen, R. Xu, X.-B. Cheng, H.-J. Peng, R. Zhang, J.-Q. Huang, Q. Zhang, Columnar lithium metal anodes, Angew. Chem. Int. Ed. 56 (2017) 14207–14211.
[34] S. Dalavi, M. Xu, B. Knight, B.L. Lucht, Effect of added LiBOB on high voltage (LiNi0.5Mn1.5O4) spinel cathodes, Electrochem. Solid State Lett. 15 (2011) A28.
[35] M. Xu, L. Zhou, L. Hao, L. Xing, W. Li, B.L. Lucht, Investigation and application of lithium difluoro(oxalate)borate (LiDFOB) as additive to improve the thermal stability of electrolyte for lithium-ion batteries, J. Power Sources 196 (2011) 6794–6801.
[36] F. Shi, A. Pei, A. Vailionis, J. Xie, B. Liu, J. Zhao, Y. Gong, Y. Cui, Strong texturing of lithium metal in batteries, Proc. Natl. Acad. Sci. 114 (2017) 12138–12143.
[37] J. Guo, Z. Wen, M. Wu, J. Jin, Y. Liu, Vinylene carbonate–$LiNO_3$: a hybrid additive in carbonic ester electrolytes for SEI modification on Li metal anode, Electrochem. Commun. 51 (2015) 59–63.

[38] G. Jiang, F. Li, H. Wang, M. Wu, S. Qi, X. Liu, S. Yang, J. Ma, Perspective on high-concentration electrolytes for lithium metal batteries, Small Struct. 2 (2021) 2000122.

[39] S. Chen, J. Zheng, D. Mei, K.S. Han, M.H. Engelhard, W. Zhao, W. Xu, J. Liu, J.-G. Zhang, High-voltage lithium-metal batteries enabled by localized high-concentration electrolytes, Adv. Mater. 30 (2018) 1706102.

[40] D.-J. Yoo, S. Yang, K.J. Kim, J.W. Choi, Fluorinated aromatic diluent for high-performance lithium metal batteries, Angew. Chem. Int. Ed. 59 (2020) 14869–14876.

[41] J.Z. Lee, T.A. Wynn, M.A. Schroeder, J. Alvarado, X. Wang, K. Xu, Y.S. Meng, Cryogenic focused ion beam characterization of lithium metal anodes, ACS Energy Lett. 4 (2019) 489–493.

[42] W. Shin, A. Manthiram, A facile potential hold method for fostering an inorganic solid-electrolyte interphase for anode-free lithium-metal batteries, Angew. Chem. 134 (2022) e202115909.

[43] Y. Tang, L. Zhang, J. Chen, H. Sun, T. Yang, Q. Liu, Q. Huang, T. Zhu, J. Huang, Electro-chemo-mechanics of lithium in solid state lithium metal batteries, Energy Environ. Sci. 14 (2021) 602–642.

[44] K.B. Hatzell, X.C. Chen, C.L. Cobb, N.P. Dasgupta, M.B. Dixit, L.E. Marbella, M. T. McDowell, P.P. Mukherjee, A. Verma, V. Viswanathan, A.S. Westover, W. G. Zeier, Challenges in lithium metal anodes for solid-state batteries, ACS Energy Lett. 5 (2020) 922–934.

[45] P. Wang, W. Qu, W.-L. Song, H. Chen, R. Chen, D. Fang, Electro–chemo–mechanical issues at the interfaces in solid-state lithium metal batteries, Adv. Funct. Mater. 29 (2019) 1900950.

[46] B.S. Vishnugopi, K.G. Naik, H. Kawakami, N. Ikeda, Y. Mizuno, R. Iwamura, T. Kotaka, K. Aotani, Y. Tabuchi, P.P. Mukherjee, Asymmetric contact loss dynamics during plating and stripping in solid-state batteries, Adv. Energy Mater. 13 (2023) 2203671.

[47] T. Krauskopf, F.H. Richter, W.G. Zeier, J. Janek, Physicochemical concepts of the lithium metal anode in solid-state batteries, Chem. Rev. 120 (2020) 7745–7794.

[48] A. Mistry, P.P. Mukherjee, Molar volume mismatch: a malefactor for irregular metallic electrodeposition with solid electrolytes, J. Electrochem. Soc. 167 (2020) 082510.

[49] D. Chatterjee, K.G. Naik, B.S. Vishnugopi, P.P. Mukherjee, Electrodeposition stability landscape for solid–solid interfaces, Adv. Sci. 11 (2024) 2307455.

[50] C. Monroe, J. Newman, The impact of elastic deformation on deposition kinetics at lithium/polymer interfaces, J. Electrochem. Soc. 152 (2005) A396.

[51] C. Monroe, J. Newman, The effect of interfacial deformation on electrodeposition kinetics, J. Electrochem. Soc. 151 (2004) A880.

[52] J.A. Lewis, J. Tippens, F.J.Q. Cortes, M.T. McDowell, Chemo-mechanical challenges in solid-state batteries, Trends Chem. 1 (2019) 845–857.

[53] Y. Ren, Y. Shen, Y. Lin, C.-W. Nan, Direct observation of lithium dendrites inside garnet-type lithium-ion solid electrolyte, Electrochem. Commun. 57 (2015) 27–30.

[54] Z. Ning, G. Li, D.L.R. Melvin, Y. Chen, J. Bu, D. Spencer-Jolly, J. Liu, B. Hu, X. Gao, J. Perera, C. Gong, S.D. Pu, S. Zhang, B. Liu, G.O. Hartley, A.J. Bodey, R. I. Todd, P.S. Grant, D.E.J. Armstrong, T.J. Marrow, C.W. Monroe, P.G. Bruce, Dendrite initiation and propagation in lithium metal solid-state batteries, Nature 618 (2023) 287–293.

[55] Z. Ahmad, V. Viswanathan, Stability of electrodeposition at solid-solid interfaces and implications for metal anodes, Phys. Rev. Lett. 119 (2017) 056003.

[56] T. Krauskopf, F.H. Richter, W.G. Zeier, J. Janek, Physicochemical concepts of the lithium metal anode in solid-state batteries, Chem. Rev. 120 (2020) 7745–7794.

[57] X. Zhang, Q.J. Wang, K.L. Harrison, S.A. Roberts, S.J. Harris, Pressure-driven interface evolution in solid-state lithium metal batteries, Cell Rep. Phys. Sci. 1 (2020) 100012.

[58] C. Hänsel, D. Kundu, The stack pressure dilemma in sulfide electrolyte based li metal solid-state batteries: a case study with Li6PS5Cl solid electrolyte, Adv. Mater. Interfac. 8 (2021) 2100206.

[59] J.-M. Doux, H. Nguyen, D.H.S. Tan, A. Banerjee, X. Wang, E.A. Wu, C. Jo, H. Yang, Y.S. Meng, Stack pressure considerations for room-temperature all-solid-state lithium metal batteries, Adv. Energy Mater. 10 (2020) 1903253.

[60] L. Porz, T. Swamy, B.W. Sheldon, D. Rettenwander, T. Frömling, H.L. Thaman, S. Berendts, R. Uecker, W.C. Carter, Y. Chiang, Mechanism of lithium metal penetration through inorganic solid electrolytes, Adv. Energy Mater. 7 (2017) 1701003.

[61] W.S. LePage, Y. Chen, E. Kazyak, K.-H. Chen, A.J. Sanchez, A. Poli, E.M. Arruda, M.D. Thouless, N.P. Dasgupta, Lithium mechanics: roles of strain rate and temperature and implications for lithium metal batteries, J. Electrochem. Soc. 166 (2019) A89.

[62] B. Hu, S. Zhang, Z. Ning, D. Spencer-Jolly, D.L.R. Melvin, X. Gao, J. Perera, S. D. Pu, G.J. Rees, L. Wang, L. Yang, H. Gao, S. Marathe, G. Burca, T.J. Marrow, P. G. Bruce, Deflecting lithium dendritic cracks in multi-layered solid electrolytes, Joule 8 (2024) 2623–2638.

[63] T. Cao, R. Xu, X. Cheng, M. Wang, T. Sun, J. Lu, X. Liu, Y. Zhang, Z. Zhang, Chemomechanical origins of the dynamic evolution of isolated Li filaments in inorganic solid-state electrolytes, Nano Lett. 24 (2024) 1843–1850.

[64] F. Aguesse, W. Manalastas, L. Buannic, J.M. Lopez del Amo, G. Singh, A. Llordés, J. Kilner, Investigating the dendritic growth during full cell cycling of garnet electrolyte in direct contact with Li metal, ACS Appl. Mater. Interfaces 9 (2017) 3808–3816.

[65] Y. Song, L. Yang, W. Zhao, Z. Wang, Y. Zhao, Z. Wang, Q. Zhao, H. Liu, F. Pan, Revealing the short-circuiting mechanism of garnet-based solid-state electrolyte, Adv. Energy Mater. 9 (2019) 1900671.

[66] W. Yu, N. Deng, Y. Feng, X. Feng, H. Xiang, L. Gao, B. Cheng, W. Kang, K. Zhang, Understanding multi-scale ion-transport in solid-state lithium batteries, eScience 5 (2025) 100278.

[67] Q. Wu, S. Xiong, F. Li, A. Matic, Electro-chemo-mechanical failure mechanisms of solid-state electrolytes, Batter. Supercaps 6 (2023) e202300321.

[68] S. Wenzel, T. Leichtweiss, D. Krüger, J. Sann, J. Janek, Interphase formation on lithium solid electrolytes—an *in situ* approach to study interfacial reactions by photoelectron spectroscopy, Solid State Ionics 278 (2015) 98–105.

[69] C. Lee, S.Y. Han, J.A. Lewis, P.P. Shetty, D. Yeh, Y. Liu, E. Klein, H.-W. Lee, M. T. McDowell, Stack pressure measurements to probe the evolution of the lithium–solid-state electrolyte interface, ACS Energy Lett. 6 (2021) 3261–3269.

[70] T. Nakamura, K. Amezawa, J. Kulisch, W.G. Zeier, J. Janek, Guidelines for all-solid-state battery design and electrode buffer layers based on chemical potential profile calculation, ACS Appl. Mater. Interfaces 11 (2019) 19968–19976.

[71] X. Fan, X. Ji, F. Han, J. Yue, J. Chen, L. Chen, T. Deng, J. Jiang, C. Wang, Fluorinated solid electrolyte interphase enables highly reversible solid-state Li metal battery, Sci. Adv. 4 (2018) eaau9245.

[72] S. Lee, K. Lee, S. Kim, K. Yoon, S. Han, M.H. Lee, Y. Ko, J.H. Noh, W. Kim, K. Kang, Design of a lithiophilic and electron-blocking interlayer for dendrite-free lithium-metal solid-state batteries, Sci. Adv. 8 (2022) eabq0153.

[73] C.-T. Yang, Y. Qi, Maintaining a flat li surface during the Li stripping process via interface design, Chem. Mater. 33 (2021) 2814–2823.

[74] Z. Deng, X. Lin, Z. Huang, J. Meng, Y. Zhong, G. Ma, Y. Zhou, Y. Shen, H. Ding, Y. Huang, Recent progress on advanced imaging techniques for lithium-ion batteries, Adv. Energy Mater. 11 (2021) 2000806.

[75] A. Dutta, S. Matsuda, Application of noninvasive imaging techniques for high energy density lithium metal rechargeable batteries, Batter. Supercaps 8 (2025) e202400504.

[76] P. Ji, X. Lei, D. Su, *In situ* transmission electron microscopy methods for lithium-ion batteries, Small Methods 8 (2024) 2301539.

[77] T. Foroozan, S. Sharifi-Asl, R. Shahbazian-Yassar, Mechanistic understanding of Li dendrites growth by *in- situ/operando* imaging techniques, J. Power Sources 461 (2020) 228135.

[78] Z. Sun, M. Li, B. Xiao, X. Liu, H. Lin, B. Jiang, H. Liu, M. Li, D.-L. Peng, Q. Zhang, *In situ* transmission electron microscopy for understanding materials and interfaces challenges in all-solid-state lithium batteries, eTransportation 14 (2022) 100203.

[79] Y. Lin, M. Zhou, X. Tai, H. Li, X. Han, J. Yu, Analytical transmission electron microscopy for emerging advanced materials, Matter 4 (2021) 2309–2339.

[80] F. Orsini, A. Du Pasquier, B. Beaudoin, J.M. Tarascon, M. Trentin, N. Langenhuizen, E. De Beer, P. Notten, *In situ* Scanning Electron Microscopy (SEM) observation of interfaces within plastic lithium batteries, J. Power Sources 76 (1998) 19–29.

[81] F. Orsini, A. du Pasquier, B. Beaudouin, J.M. Tarascon, M. Trentin, N. Langenhuizen, E. de Beer, P. Notten, *In situ* SEM study of the interfaces in plastic lithium cells, J. Power Sources 81–82 (1999) 918–921.

[82] G. Rong, X. Zhang, W. Zhao, Y. Qiu, M. Liu, F. Ye, Y. Xu, J. Chen, Y. Hou, W. Li, W. Duan, Y. Zhang, Liquid-phase electrochemical scanning electron microscopy for *in situ* investigation of lithium dendrite growth and dissolution, Adv. Mater. 29 (2017) 1606187.

[83] C. Cui, H. Yang, C. Zeng, S. Gui, J. Liang, P. Xiao, S. Wang, G. Huang, M. Hu, T. Zhai, H. Li, Unlocking the *in situ* Li plating dynamics and evolution mediated by diverse metallic substrates in all-solid-state batteries, Sci. Adv. 8 (2022) eadd2000.

[84] Q. Chen, C. Dwyer, G. Sheng, C. Zhu, X. Li, C. Zheng, Y. Zhu, Imaging beam-sensitive materials by electron microscopy, Adv. Mater. 32 (2020) 1907619.

[85] F. Lin, I.M. Markus, M.M. Doeff, H.L. Xin, Chemical and structural stability of lithium-ion battery electrode materials under electron beam, Sci. Rep. 4 (2014) 5694.

[86] S. Weng, Y. Li, X. Wang, Cryo-EM for battery materials and interfaces: workflow, achievements, and perspectives, iScience 24 (2021) 103402.

[87] M.J. Zachman, Z. Tu, L.A. Archer, L.F. Kourkoutis, Nanoscale elemental mapping of intact solid–liquid interfaces and reactive materials in energy devices enabled by cryo-FIB/SEM, ACS Energy Lett. 5 (2020) 1224–1232.

[88] O.O. Taiwo, D.P. Finegan, J.M. Paz-Garcia, D.S. Eastwood, A.J. Bodey, C. Rau, S. A. Hall, D.J.L. Brett, P.D. Lee, P.R. Shearing, Investigating the evolving microstructure of lithium metal electrodes in 3D using X-ray computed tomography, Phys. Chem. Chem. Phys. 19 (2017) 22111–22120.

[89] F. Lin, Y. Liu, X. Yu, L. Cheng, A. Singer, O.G. Shpyrko, H.L. Xin, N. Tamura, C. Tian, T.-C. Weng, X.-Q. Yang, Y.S. Meng, D. Nordlund, W. Yang, M.M. Doeff, Synchrotron X-ray analytical techniques for studying materials electrochemistry in rechargeable batteries, Chem. Rev. 117 (2017) 13123–13186.

[90] J. Le Houx, D. Kramer, X-ray tomography for lithium ion battery electrode characterisation — a review, Energy Rep. 7 (2021) 9–14.

[91] F. Tang, Z. Wu, C. Yang, M. Osenberg, A. Hilger, K. Dong, H. Markötter, I. Manke, F. Sun, L. Chen, G. Cui, Synchrotron X-ray tomography for rechargeable battery research: fundamentals, setups and applications, Small Methods 5 (2021) 2100557.

[92] D.S. Eastwood, P.M. Bayley, H.J. Chang, O.O. Taiwo, J. Vila-Comamala, D.J. L. Brett, C. Rau, P.J. Withers, P.R. Shearing, C.P. Grey, P.D. Lee, Three-dimensional characterization of electrodeposited lithium microstructures using synchrotron X-ray phase contrast imaging, Chem. Commun. 51 (2014) 266–268.

[93] F. Sun, L. Zielke, H. Markötter, A. Hilger, D. Zhou, R. Moroni, R. Zengerle, S. Thiele, J. Banhart, I. Manke, Morphological evolution of electrochemically plated/stripped lithium microstructures investigated by synchrotron X-ray phase contrast tomography, ACS Nano 10 (2016) 7990–7997.

[94] O.O. Taiwo, D.P. Finegan, J.M. Paz-Garcia, D.S. Eastwood, A.J. Bodey, C. Rau, S. A. Hall, D.J.L. Brett, P.D. Lee, P.R. Shearing, Investigating the evolving

microstructure of lithium metal electrodes in 3D using X-ray computed tomography, Phys. Chem. Chem. Phys. 19 (2017) 22111–22120.
[95] F. Shen, M.B. Dixit, X. Xiao, K.B. Hatzell, Effect of pore connectivity on li dendrite propagation within llzo electrolytes observed with synchrotron X-ray tomography, ACS Energy Lett. 3 (2018) 1056–1061.
[96] M.B. Dixit, A. Verma, W. Zaman, X. Zhong, P. Kenesei, J.S. Park, J. Almer, P. P. Mukherjee, K.B. Hatzell, Synchrotron imaging of pore formation in Li metal solid-state batteries aided by machine learning, ACS Appl. Energy Mater. 3 (2020) 9534–9542.
[97] J.A. Lewis, F.J.Q. Cortes, Y. Liu, J.C. Miers, A. Verma, B.S. Vishnugopi, J. Tippens, D. Prakash, T.S. Marchese, S.Y. Han, C. Lee, P.P. Shetty, H.-W. Lee, P. Shevchenko, F. De Carlo, C. Saldana, P.P. Mukherjee, M.T. McDowell, Linking void and interphase evolution to electrochemistry in solid-state batteries using operando X-ray tomography, Nat. Mater. 20 (2021) 503–510.
[98] H. Nozaki, H. Kondo, T. Shinohara, D. Setoyama, Y. Matsumoto, T. Sasaki, K. Isegawa, H. Hayashida, *In situ* neutron imaging of lithium-ion batteries during heating to thermal runaway, Sci. Rep. 13 (2023) 22082.
[99] S. Wang, H. Shi, D. Wang, Y. Xia, Y. Yin, S. Liang, Y. Hu, R. Shao, X. Wu, Z. Xu, Neutron-based characterization: a rising star in illuminating rechargeable lithium metal batteries, Nano Energy 122 (2024) 109337.
[100] R. Bradbury, N. Kardjilov, G.F. Dewald, A. Tengattini, L. Helfen, W.G. Zeier, I. Manke, Visualizing lithium ion transport in solid-state Li–S batteries using ^{6}Li contrast enhanced neutron imaging, Adv. Funct. Mater. 33 (2023) 2302619.
[101] T. Famprikis, P. Canepa, J.A. Dawson, M.S. Islam, C. Masquelier, Fundamentals of inorganic solid-state electrolytes for batteries, Nat. Mater. 18 (2019) 1278–1291.
[102] J. Yang, F. Mo, J. Hu, S. Li, L. Huang, F. Fang, D. Sun, G. Sun, F. Wang, Y. Song, Revealing the dynamic evolution of Li filaments within solid electrolytes by operando small-angle neutron scattering, Appl. Phys. Lett. 121 (2022) 163901.
[103] P.P. Mukherjee, S. Pannala, J.A. Turner, Modeling and simulation of battery systems, in: C. Daniel, J.O. Besenhard (Eds.), Handb. Battery Mater, 2011, pp. 841–875.
[104] A.Y.S. Eng, C.B. Soni, Y. Lum, E. Khoo, Z. Yao, S.K. Vineeth, V. Kumar, J. Lu, C. S. Johnson, C. Wolverton, Z.W. Seh, Theory-guided experimental design in battery materials research, Sci. Adv. 8 (2022) eabm2422.
[105] M.T. Castro, J.A.D. Del Rosario, M.N. Chong, P.-Y.A. Chuang, J. Lee, J.D. Ocon, Multiphysics modeling of lithium-ion, lead-acid, and vanadium redox flow batteries, J. Energy Storage 42 (2021) 102982.
[106] A. De Gol, K.B. Dermenci, L. Farkas, M. Berecibar, Electro-chemo-mechanical degradation in solid-state batteries: a review of microscale and multiphysics modeling, Adv. Energy Mater. 14 (2024) 2403255.
[107] H. Yang, X. Li, K. Fu, W. Shang, K. Sun, Z. Yang, G. Hu, P. Tan, Behavioral description of lithium-ion batteries by multiphysics modeling, DeCarbon 6 (2024) 100076.
[108] J. Jeon, G.H. Yoon, T. Vegge, J.H. Chang, Phase-field investigation of lithium electrodeposition at different applied overpotentials and operating temperatures, ACS Appl. Mater. Interfaces 14 (2022) 15275–15286.
[109] J.O. Dow, Introduction to problem definition and development, in: J.O. Dow (Ed.), A Unified Approach Finite Elem. Method Error Anal. Proced., Academic Press, 1999, pp. 1–8.
[110] C.H. Forsberg, Chapter 5 - numerical methods (steady and unsteady), in: C. H. Forsberg (Ed.), Heat Transf. Princ. Appl., Academic Press, 2021, pp. 163–210.
[111] Y. Liu, X. Xu, X. Jiao, O.O. Kapitanova, Z. Song, S. Xiong, Role of interfacial defects on electro–chemo–mechanical failure of solid-state electrolyte, Adv. Mater. 35 (2023) 2301152.
[112] S. Xiong, X. Xu, X. Jiao, Y. Wang, O.O. Kapitanova, Z. Song, Y. Liu, Mechanical failure of solid-state electrolyte rooted in synergy of interfacial and internal defects, Adv. Energy Mater. 13 (2023) 2203614.
[113] X. Xu, Y. Liu, O.O. Kapitanova, Z. Song, J. Sun, S. Xiong, Electro–chemo–mechanical failure of solid electrolytes induced by growth of internal lithium filaments, Adv. Mater. 34 (2022) 2207232.